March 2020

Laser-Induced Breakdown Spectroscopy for Elemental Analysis in Bioarchaeology and Forensic Anthropology

Kelsi N. Kuehn
University of South Florida

Laser-Induced Breakdown Spectroscopy for Elemental Analysis in Bioarchaeology and Forensic Anthropology

by

Kelsi N. Kuehn

A thesis submitted in partial fulfillment
of the requirements for the degree of
Master of Arts
Department of Anthropology
College of Arts and Sciences
University of South Florida

Major Professor: Jonathan Bethard, Ph.D., D-ABFA
Elizabeth Miller, Ph.D.
Matthieu Baudelet, Ph.D.

Date of Approval:
March 24, 2020

Keywords: osteology, commingling, human skeletal analysis

ACKNOWLEDGMENTS

I would like to thank Dr. Matthieu Baudelet and the research team at the National Center for Forensic Science at UCF for giving me access to the LIBS instrument and for helping me with the chemistry side of this project. I would also like to thank Dr. Erin Kimmerle for granting me permission to use the donated skeletal collection at the Institute of Forensic and Applied Science at USF. Many thanks go to Dr. Jonathan Bethard for his continued support and encouragement throughout this project. A big thank you to Dr. Elizabeth Miller for pushing me to think bigger, and to Dr. Christian Wells for all of his assistance with the statistics required to complete this project. Finally, I would like to thank all of my friends and loved ones, especially those in the USF Anthropology Department, who stood by me not only during this thesis-writing process, but along my journey through graduate school. To my roommates, Jonny and Paj (and Atticus), I appreciate your relentless positivity, unwavering support, and for putting up with me all this time.

TABLE OF CONTENTS

LIST OF TABLES

LIST OF FIGURES

LIST OF ABBREVIATIONS

ANOVA ..... analysis of variance

CT ..... computed tomography

DFA ..... discriminant function analysis

DNA ..... deoxyribonucleic acid

EDX ..... energy dispersive X-ray

FTIR ..... Fourier transform infrared spectroscopy

HH LIBS ..... handheld laser-induced breakdown spectroscopy

ICP ..... inductively coupled plasma

ICP-OES ..... inductively coupled plasma optical emission spectrometry

ICP-MS ..... inductively coupled plasma-mass spectrometry

IFAAS ..... Institute of Forensic and Applied Science

LA-ICP-MS ..... laser ablation-inductively coupled plasma-mass spectrometry

LA-ICP-SF-MS ..... laser ablation-inductively coupled plasma-sector field mass spectrometry

LIBS ..... laser-induced breakdown spectroscopy

MANOVA ..... multivariate analysis of variance

MRI ..... magnetic resonance imaging

Nd:YAG ..... neodymium-doped yttrium aluminum garnet

NIR ..... near infrared

PCA ..... principal component analysis

PLS-DA ..... partial least squares discriminant analysis

ppm ..... parts per million

pRIA..... protein radioimmunoassay

pXRF..... portable X-ray fluorescence

SEM ..... scanning electron microscopy

SEM-EDS ..... scanning electron microscopy-energy dispersive spectroscopy

XRF..... X-ray fluorescence

XRD ..... X-ray diffraction

LIST OF CHEMICAL SYMBOLS

Ag.....Silver
Al..... Aluminum
B.....Boron
Ba .....Barium
Be ..... Beryllium
Br.....Bromine
C.....Carbon
Ca .....Calcium
Cl.....Chlorine
Co.....Cobalt
Cr..... Chromium
Cu.....Copper
F .....Fluorine
Fe.....Iron
H.....Hydrogen
K..... Potassium
Li .....Lithium
Mg.....Magnesium
Mn..... Manganese
N..... Nitrogen
Na..... Sodium
Nd.....Neodymium
Ni.....Nickel
O.....Oxygen
P .....Phosphorus
Pb .....Lead
Rb.....Rubidium
S .....Sulfur
Si ..... Silicon
Sr.....Strontium
Ti .....Titanium
Zn ..... Zinc

ABSTRACT

Within bioarchaeology and forensic anthropology, the current processes of differentiating between individual human skeletal remains are imprecise, costly, and inefficient. A novel analytical technique within anthropology, laser-induced breakdown spectroscopy (LIBS) can aid in the identification of human remains using rapid laser ablation occurring at the micro-scale, making the technique virtually non-destructive to the sample. Considering this, LIBS could offer a superior method for materials discrimination and human identification. This research sought to examine whether LIBS can be used to obtain elemental signatures within bones to distinguish individuals from one another in a rapid, non-destructive manner. Seven human skeletal donors and two archaeological samples were analyzed with LIBS in order to test whether individuals could be distinguished from one another using elemental signatures within bones. Results showed that LIBS spectral data can be used to correctly classify individuals and archaeological samples, as well as provide information about burial environment and disposition. The application of LIBS within the fields of bioarchaeology and forensic anthropology opens new doors for rapid, non-destructive skeletal analysis, allowing anthropologists to shed new light on human variation at an elemental level.

CHAPTER ONE: INTRODUCTION

Anthropological Methods for Skeletal Analysis

Anthropology is a comprehensive and holistic discipline dedicated to the interpretation of the human condition, from the past to the present, utilizing an integrative approach through various subdisciplines such as archaeology, social and cultural anthropology, linguistics, and biological anthropology (Langley & Tersigni-Tarrant, 2017). Within the subfields of archaeology and biological anthropology, specialists like bioarchaeologists and forensic anthropologists investigate the biological aspects of humans through skeletal analysis (Gosman & Stout, 2010*)*. Human skeletal analysis plays an important role in understanding how diseases, physiological stress, trauma, physical activity, malnutrition, the environment, and other factors impact individuals during their life (Gosman & Stout, 2010*)*. Combined with an understanding of human skeletal growth and development, variation, and degeneration, such factors provide biological clues about an individual (Langley & Tersigni-Tarrant, 2017). These clues help investigators estimate four key characteristics: age, sex, ancestry, and stature, more commonly referred to as the biological profile, which narrow the search parameters when identifying a deceased person (Stewart, 1979; Blau & Ubelaker, 2016).

For more than a century, practitioners have developed and utilized a variety of methods to estimate aspects of the biological profile, many of which have greatly improved over the last few decades thanks to the advancement of technology (Dirkmaat & Cabo, 2012; Ross & Kimmerle, 2009; Ubelaker, 2018; Fakiha, 2019). For example, traditional methods consisted of

measuring bones and features by hand, identifying samples visually using comparative morphology, and basic statistical analyses using limited sample sizes (Ross & Kimmerle, 2009; Dirkmaat & Cabo, 2012; Larsen, 2010; Finlayson, Bartelink, Perrone, & Dalton, 2017*)*. With technology like 3-D scanning, digitization, MRI, CT, scanning electron microscopes, facial reconstruction and recognition, stable isotope analysis, DNA analysis, and mass spectrometry, new methods are being developed to more precisely estimate age at death, living stature, region of origin, and sex in unknown individuals (Larsen, 2010; Ubelaker, 2018; Fakiha, 2019; Ross & Kimmerle, 2009). Additionally, current high-tech methods can be used to resolve other issues faced by bioarchaeologists and forensic anthropologists like identifying unknown materials, sorting and identifying individuals in commingled assemblages, and determining minimum number of individuals (MNI) or most likely number of individuals (MLNI) in a mass burial (Byrd & Adams, 2016; Finlayson et al., 2017; Osterholtz, Baustian, & Martin, 2014; Langley & Tersigni-Tarrant, 2017; Ubelaker, 2018).

In bioarchaeology and forensic anthropology, the biological profile plays an important role in understanding the individual(s) and how they may relate to the scene, whether it be a homicide from last week or a mass burial under a church from medieval Transylvania (Bethard, et al., 2019; Schultz, 2012; Osterholtz et al., 2014; Krishan et al., 2016; Gocha et al., 2014). When working with the remains of an unknown individual, estimating the parameters of the biological profile is a necessary first step (Langley & Tersigni-Tarrant, 2017; Gocha et al., 2015). In forensic cases, Ross and Kimmerle (2009) argued that developing a biological profile starting with precise sex and ancestry estimations is critical to the identification process because these parameters can narrow the search for an individual more quickly. In addition, age and stature estimations can vary depending on sex and ancestry, resulting in a less reliable biological

profile (Ross & Kimmerle, 2009; Gocha et al., 2015; Krishan et al., 2016). Similarly, in bioarchaeology, key biological attributes like age, sex, ancestry, health, and diet make up demographic profiles which aid in the analysis of commingled assemblages, allowing bioarchaeologists to better understand the circumstances surrounding the creation of the interment, as well as the life histories of those buried within (Osterholtz et al., 2014; Finlayson et al., 2017; Larsen, 2002; Cabo et al., 2012; Lambacher et al., 2016). In both instances, it is clear how informative the biological profile can be, especially when it is possible to estimate all four characteristics. So, what happens when the biological profile is inconclusive or several aspects are unknown, perhaps due to incomplete, fragmented, or disarticulated remains?

Modern Technology in Biological Anthropology

Despite the improved methodologies and advanced technology available today, most of the methods used to attain a biological profile require well-preserved remains and a mostly complete skeleton (Ubelaker, 2018; Ubelaker, 2004). In some cases, it is difficult to identify a bone fragment from other materials, let alone identify the bone or perform osteological analysis (Langley & Tersigni-Tarrant, 2017; Ubelaker, 1998; Christensen et al., 2012). A primary challenge in bioarchaeology and forensic anthropology is the differentiation of human remains from non-human remains in a rapid, yet non-destructive manner. Currently, common techniques used to identify human osseous material include radiogrammetry, histological analyses, DNA testing, and morphological or microscopic examinations (Ubelaker et al., 2002; Christensen et al., 2012; Langley & Tersigni-Tarrant, 2017; Ubelaker, 1998; Gocha et al., 2015). Unfortunately, most of these techniques are limited in their efficacy by one or more factors, including length of analysis time, access to specialized equipment, cost, destructive sample preparation, and the need

for larger sections of bone or nearly complete remains (Langley & Tersigni-Tarrant, 2017; Ubelaker, 1998; Dirkmaat & Cabo, 2012). In cases of mass disasters or commingled remains, the current process of separating osseous fragments from other materials, discriminating human remains from non-human remains, and identifying individuals from one another is simply inefficient.

Recently, bioarchaeologists and forensic anthropologists have begun using relatively non-destructive elemental analysis techniques like scanning electron microscopy with energy dispersive X-ray spectroscopy (SEM/EDS), X-ray fluorescence (XRF), laser ablation inductively coupled plasma mass spectrometry (LA-ICP-MS), Fourier-transform infrared spectroscopy (FTIR), and laser-induced breakdown spectroscopy (LIBS) (Christensen et al., 2012; Ubelaker et al., 2002; Houck, 2015; Ubelaker, 2018; Kerley, 1965; Baker, 2016; Hark, 2014; Rinke-Kneapler & Sigman, 2014; Ubelaker, 2004). These methods provide information on the elemental composition of a sample in order to determine what material it is. A brief overview of alternative elemental analytical techniques and their applications for skeletal analysis can be found in Table 1.1 below.

Table 1.1. Elemental analysis techniques used for skeletal analysis.*

Analytical Method	Purpose	Results and Observations	Selected References
SEM/EDS	Distinguish osseous tissue from other materials.	Determines whether small, fragmentary, otherwise unidentifiable evidence is consistent with osseous or dental tissue, when morphological features are not available; allows for comparison to known bone and teeth samples when used in conjunction with FBI spectral database; proportions and concentrations of Ca and P are most important discriminating factor from other materials; not likely to discriminate bone from ivory, mineral apatite, and corals due to similar composition.	Ubelaker, 2002; Fakiha, 2019
XRF/pXRF	Distinguish skeletal materials from non-bone materials, including in cases of cremation; understand diagenesis and life environmental exposure in archaeological skeletal remains.	Archaeological bone composition characterized by chemical signals related to biochemical degradation of bones, metal leaching from the soil, presence of fine silt soil particles, and lead content; highly acid soil leads to poor preservation; thoracic bones are more sensitive to diagenesis and the burial environment; osseous and dental materials could be identified based on Ca/P levels detected by XRF; mineral apatite, octocoral, and brachiopod shells Ca/P profiles are too similar to bone and tooth to discriminate, but they vary structurally; XRF detected significantly different levels of P, K, Zn, Al, and S between cremated bone and the contaminants within the cremains; pXRF able to discriminate between bone and nonbone material (including ivory and octocoral) at 94% using the linear relationship between Ca/P spectral and molar ratios.	Christensen, 2012; Gilpin & Christensen, 2015; Zimmerman et al., 2015; López-Costas et al., 2016
FTIR	Analyze burned bones to understand the effects on bone microstructure and pyre conditions from an archaeological context.	Direct relationship between cremation intensity (duration and temperature) and crystallinity index (CI), with an indirect relationship with C/P ratio; CI and C/P can be used to distinguish unburned bone from bone burned at varying intensities.	Squires et al., 2011

**LIBS was excluded from this table as it will be the focus of the next section.*

Laser-Induced Breakdown Spectroscopy

The following discussion focuses on the application of LIBS in forensic anthropology and bioarchaeology as an improved method of materials discrimination and human identification. LIBS can aid in the identification of human remains using rapid laser ablation to analyze elements in a sample (Moncayo et al., 2014). With this analysis occurring at the micro-scale, the technique is virtually non-destructive to the sample and cannot typically be seen by the naked eye. Using elemental signatures in addition to ratios of certain elements (calcium, potassium, magnesium, etc.), osseous/dental fragments can be separated from non-skeletal samples. There are very few studies using LIBS in this context, as determined in a review of the current literature, however the research suggests that using LIBS for the identification of human skeletal remains is possible.

Background

When examining evidence from a crime scene or skeletal remains from an archaeological context, the analysis should be quick, cost-effective, reliable, and most importantly, minimally destructive in order to preserve as much of the sample as possible. LIBS checks all of these boxes as a laser-based analytical technique. Laser ablation works by focusing a high-powered laser pulse on a very small region of the sample's surface in order to form a plasma, which consists of excited atoms and ions produced during the ablation and vaporization of the sample (Rinke-Kneapler & Sigman, 2014; Almirall, 2010). The atomic emissions from the sample surface are collected by an optic sensor connected to a spectrometer, which essentially converts the light from the emissions into individual emission peaks called spectra, producing a visual representation of the elemental composition of the sample (Rinke-Kneapler & Sigman, 2014;

Almirall, 2017). This process takes place at a micrometer scale (1 micrometer = 0.001 mm) meaning the ablation crater on the sample surface can rarely be seen by the naked eye. Additionally, LIBS stands out among other analytical techniques due to its relatively low cost, speed of analysis, ease of operation, lack of sample preparation (regardless of gas, liquid, or solid phase), portable options for field use, and high sensitivity for many elements, including lighter (low atomic mass) elements like H, Li, Be, B and C, which other methods (i.e., XRF/pXRF) cannot detect (Rinke-Kneapler & Sigman, 2014; Almirall, 2017).

Within anthropology, LIBS has already been implemented for a variety of uses, but the application of LIBS to skeletal analysis for discrimination purposes is a novel technique. Generally, LIBS is utilized for materials analysis, characterization of solids, comparison analysis, and identification of materials like explosives, soil, glass, paint, inks, bodily fluids, and fibers (Hark & East, 2014; Almirall, 2017; Rinke-Kneapler & Sigman, 2014). These methodologies have been used in both forensic and bioarchaeological contexts with great success, as shown by Moncayo et al. (2014), Kasem et al. (2014), Tofanelli et al. (2014), and Rusak et al. (2011). Due to its versatility and sensitivity, LIBS is gaining popularity in the field and shows great potential for a variety of anthropological applications, especially skeletal analysis in contexts like archaeological commingled remains or forensic cases with mass graves.

Potential for LIBS in Anthropology

Unlike numerous other analytical methods, elemental analysis defines a sample by its chemical components, providing the user with immediate insight into the sample's properties. Theoretically, any unknown sample, regardless of size, shape, color, material, etc., can be characterized using its elemental composition. The same applies to skeletal analysis of human

remains. Traditionally, the process of estimating a biological profile of an individual follows deductive reasoning in the sense that broad theories centered in human variation, growth, and development are used to estimate age, sex, ancestry, and stature based on the specific observations that can be made about the individual in question (Boyd and Boyd, 2018). The process works by excluding possibilities until the most likely combination of traits can be used to narrow the search for an individual's identity (in forensic cases).

Unfortunately, these methodologies rely on restrictive categorization of humans and presumptive statistics. For example, in the United States, ancestry is typically divided into groups like "white," "black," "Hispanic/Latinx," "Native American," etc., drastically reducing the chances that an individual is classified in the same way that they identified in life, or how family and friends would recognize them (Langley & Tersigni-Terrant, 2017). As previously mentioned, some aspects of the biological profile yield "better" results when sex and/or ancestry is known, meaning the entire process relies on being able to place people in ill-fitting boxes (Ross & Kimmerle, 2009). This is not an effective method for discriminating between individuals and identifying remains, especially in a forensic context. LIBS would completely reverse this process, breaking samples down into the most basic universal chemical building blocks, which can then be used to create an individual elemental profile. Elemental analysis has the ability to circumvent the issue of defining people by ancestry, gender, or another limiting factor, potentially providing an answer to a question many anthropologists have begun asking. Beyond its use for individual discrimination, skeletal analysis with LIBS opens the door to a greater understanding of human variation at the most elementary level.

The purpose of this project is to answer the following questions through a methodological study:

1. **Can individuals be distinguished from one another using LIBS to obtain elemental signatures within bones?**
2. **Can LIBS be considered an improvement over current methods for skeletal analysis in bioarchaeology and forensic anthropology?**

The remainder of this paper presents an in-depth review of the literature, including sources outside of biological anthropology, the materials utilized and methods followed in the study, the results, and a discussion of the results and their implications for applied anthropology.

Chapter 2 provides background for the study through a discussion of the elemental composition of bone, the function of these elements in the bone, and what these elements could mean for human variation at an elemental level. Furthermore, a review of studies utilizing elemental analysis techniques to evaluate the composition of bones is provided and divided into sections by subject matter. For instance, research on cremated and burned remains is presented alongside studies involving the resolution of commingled remains and elemental analysis of archaeological samples. The final sections include research committed to answering two questions commonly asked in biological anthropology: is it bone or not? And is it human or non-human?

Chapter 3 presents the research design of the study including the samples, tools, and methodology. Tables offer summaries of donor profiles from the human skeletal sample and the elemental lines selected for analysis from the spectra. Figures are provided showing examples of spectral data, the skeletal elements analyzed during the project, and the handheld LIBS instrument. The reasoning behind the selection of specific elemental peaks is outlined through

data exploration methods and shown using a box plot and discriminant function plots. Finally, the additional statistical analyses performed on the data is introduced.

Chapter 4 provides the results from the statistical analyses performed on the elemental data obtained from LIBS. The results offer answers to several questions asked during the data analysis process. First, can the donors be separated from one another using relative elemental intensities from their skeletons? Second, can an extra rib recovered with one of the donors be reassigned to its owner? And third, can the donors be grouped by burial environment or disposition based on their elemental signatures?

Chapter 5 offers a discussion of the results, limitations encountered during elemental analysis of human skeletal remains, and implications for applied anthropology. The results are interpreted in order to better understand which factors influenced the data and what this means for future research. The limitations are presented with the design of additional studies in mind to address the potential issues researchers may face when performing elemental analysis on skeletal remains. Additionally, this study and its results are discussed regarding its impact within applied anthropology. Finally, the conclusion addresses whether this project successfully answered the two questions posed above.

CHAPTER TWO: LITERATURE REVIEW

Elemental Composition of Bone

In order to understand whether LIBS is an effective method for identifying individuals based on elemental bone composition, several questions must first be addressed: What is bone made of? Which elements are found in the human body? Do those elements serve a purpose in skeletal biology and human variation?

What is bone?

Bone is a living tissue made of both organic and inorganic components in addition to water (Kendall et al., 2018). The organic portion consists of collagen, a fibrous protein that provides a strong, flexible framework for the inorganic minerals to develop around. A specific form of calcium phosphate called hydroxyapatite is the mineral compound that forms the rigid bone matrix, adding stability and strength to the bone. The chemical formula for hydroxyapatite, $Ca_{10}(PO_4)_6(OH)_2$, indicates that the basic elemental composition of bone consists of calcium (Ca), phosphorus (P), oxygen (O), and hydrogen (H). These four elements will form the basis of the discussion on which elements may contribute to variation between individuals.

From the calcium hydroxyapatite chemical formula, it is easily determined that the stoichiometric ratio of calcium to phosphorus is 5:3, or 1.67 (Lee et al., 2006). Within human bone however, the Ca/P ratio ranges from 1.37 to 1.87, due to the complex nature of bone mineral and the presence of additional ions like Mg^{2+}, carbonate (CO_3^{2-}), and K^+ (Lee et al.,

2006). This ratio is important because other mineralized tissues in the body like dentine, cementum, and enamel are also made of collagen, hydroxyapatite, and water, but in different proportions (Kendall et al., 2018). In addition, collagen and calcium phosphate are the principal components of antler, shell, chitin, ivory, coral, and some types of rocks (Ubelaker et al., 2002; Zimmerman et al., 2015).

This compounds the issue of identifying unknown fragments because prior techniques used to sort bone from non-bone rely on major elements to identify the material (i.e., Ca, P, O, H in bone), meaning these methods cannot discriminate between materials with a similar chemical composition to bone and teeth (Zimmerman et al., 2015). In these situations, it is common to employ additional analytical techniques which may be even more destructive, time-consuming, or expensive than the initial analysis. Because of this, it is important to look at both the major elements and the trace elements within bone instead of limiting the discriminatory analysis to a comparison of Ca/P ratios (Zimmerman et al., 2015). Trace elements are more likely to be associated with environmental factors like pollution, water sources, and dietary habits, meaning they may vary to a greater extent between individuals, potentially providing the key to discrimination. Ultimately, future studies should acquire as much data as possible from a variety of samples in order to assess which elements are best for discrimination purposes and to better understand the role certain elements play in human variation.

What other elements are found in the human body?

If the ability to discriminate bone from non-bone or one individual from another cannot be accomplished using only the major elements in collagen and hydroxyapatite, what other elements in the body could be used? Trace elements are essential for human development and

their composition in bones can vary widely depending on mineral uptake in an individual's diet and environmental exposure (Castro et al., 2010). For example, Fe, Al, and Mg concentrations within bones can increase due to exogenous mineral contribution from the environment. The growth and development of bones utilizes minor and trace elements like Zn, Cr, Cu, Mn, Fe, and Mg.

In addition, previous studies have shown that the distribution of trace elements may vary according to bone structure and function (Castro et al., 2010). The structure of bone is divided into two types: cortical (dense, outer bone) or trabecular (inner spongy bone). Cortical bone regenerates more slowly than trabecular bone, making it less susceptible to environmental changes, and is the preferred bone type for elemental analysis due to its dense structure. Using multivariate statistical analyses combined with LA-ICP-SF-MS, Castro et al. (2010) determined that there are significant differences for Sr, Rb, Mg, and Fe between individuals, as well as significant differences between the humerus and femur for Ba, Pb, Mg, Al, Mn, Fe, Cu, Rb, and Sr. Other studies reported similar findings, namely Moncayo et al. (2014), which had the most success with individual discrimination using LIBS to analyze Ca, Sr, and Mg signals in bone. This list can be used as a baseline for understanding which elements may indicate human variation at the elemental level.

What do these elements mean for human variation?

With a greater understanding of which elements to focus on, it can now be asked what these elements do and how they relate to skeletal biology and human variation. As previously discussed, most of these elements are the basic building blocks of bone tissue, with the minor and trace elements playing a role in the growth and development of bone over time. There is

evidence to suggest that some elemental compositions change over time, or that the ratios between some elements indicate sex, age, or species differences.

Balatsoukas et al. (2010), examined how age, sex, and bone type affected the composition of Ca and P in rat bones since, according to the authors, changing Ca/P ratios can be an indicator of human bone health. Utilizing auger electron spectroscopy, cortical sections were analyzed from the right femora, and right front and back tibiae of 40 Wistar rats, along with trabecular sections of ribs. Results showed that the Ca/P ratio across all sites is not sex dependent, and femoral sections of bone demonstrated higher ratios of Ca/P than in the tibias. In addition, age-related changes in Ca/P levels were evident in regions of cortical bone, while the ratios in trabecular bone exhibited no sex- or age-related changes. This finding is consistent with a prior study which showed age, sex, ethnicity, and skeletal site had no impact on bone mineralization density of trabecular bone in adult humans, as seen with backscattered electron imaging.

Other studies have argued that there are elemental sex differences, specifically in the concentrations of Fe, Cu, and Zn. Jaouen et al. (2012) analyzed the stable isotope concentrations of Cu, Fe, and Zn in human hand phalanges from an archaeological context to look for a relationship to biological sex. According to the authors, modern samples of men's blood appeared Fe-depleted and Cu-enriched compared to the modern samples of women's blood. Since bones are fed nutrients through the blood supply, it was hypothesized that these differences would carry over to the skeleton. The results from the elemental analysis confirmed that male bone was Fe-depleted and Cu-enriched, relative to the female bone. In terms of assigning sex to unknown individuals, the authors were able to correctly assign 77% of bone samples using the

ratios of Fe and Cu stable isotopes, which is comparable to previous studies using this method to assign sex using blood samples (81% correct assignment rate).

Similarly, Nganvongpanit et al. (2016a) studied the feasibility of sex identification of human bone based on differences in elemental profiles. The study looked at the cranium, humerus, and os coxae of 30 male and 30 female skeletons. Using discriminant analysis, it was found that S, Ca, and Pb had significantly higher proportions in male crania, while Si, Ag, Mn, Fe, Zn, and the lighter elements (atomic number less than 12) were higher in females. In the humerus and os coxae, nine elements were significantly higher in males, while only one element was higher in females. The authors concluded that there are elemental differences between males and females, even though the accuracy rate for sex estimation using this method (60-67%) was lower than general morphological analyses.

Finally, in another study by Nganvongpanit et al. (2016b), the aim was to determine elemental profiles in bones from four mammal species (human, dog, elephant, and dolphin), to study species discrimination. The authors used discriminant analysis to determine that the combination of Ca/P + Ca/Zn + Ca/Pb + Ca/Fe + Ca/Sr + Zn/Fe could be used to successfully classify six species (dog, pig, goat, tapir, monkey, and elephant) out of 15 at a 100% accuracy rate. The study concluded with the assertion that elemental compositions can be used for species identification, especially when attempting to distinguish human from non-human bones.

Elemental Analysis of Bone

As previously discussed, determining whether an unknown material is skeletal or not becomes more difficult when the sample is fragmented, taphonomically modified, or found out of context (Ubelaker, 2004). Gross analysis of a fragment includes looking for osseous

landmarks (easily identifiable features found on each bone), taking measurements, and trying to match the unknown fragment to known samples (Finalyson et al., 2017; Ubelaker, 2018). This section intends to provide an overview of some of the elemental analytical techniques found in the current literature.

To begin, Brätter et al. (1977) studied the use of instrumental neutron activation analysis and flameless atomic absorption spectrometry as a medical diagnostic aid. The team took data from 69 well preserved ancient human skeletons in order to understand the distribution of elements throughout the skeleton. Multiple sampling sites were chosen on the long bones, clavicles, ribs, lumbar vertebra, and calcaneus were selected for data collection, for a total of 80 sites. Separate data was taken from the iliac crest on the innominate bones because of its relevance in biopsies. The methods used in this study are traditional forms of spectrometry, but effective for detecting multiple elements simultaneously. The results showed that 25 trace elements have a varied distribution within one bone, and their distribution throughout the entire skeleton are related to the functional and structural characteristics near the sampling sites. Higher concentrations of elements were observed in epiphyseal areas of long bones, as opposed to the shafts, as well as in trabecular bone versus cortical bone. Finally, the elements F, Pb, Sr, and Zn were determined to be of medical significance to the study of health problems in humans due to their relationship to bone tissue.

Kosugi et al. (1986) used ICP atomic emission spectrometry and atomic absorption spectrometry to analyze the elemental composition of ancient Japanese bones. Excavated rib bones from 50 sites across Japan were analyzed to measure the concentration of 19 elements. The authors were able to classify 141 specimens into five groups based on Japanese prehistoric and historic eras (Jomon, Yayoi, Kofun, Kamakura, and Muromachi). Al, B, and Cr showed no

significant changes across eras, and the average concentrations of Ca and P indicated the specimens were well-preserved. In the Edo group, the Ca/P molar ratios were the lowest, but concentrations of Pb, Fe, Co, and Mn were all elevated compared to other groups. Furthermore, specimens from the Kofun group showed the highest levels of Cd, Zn, and Mg and the lowest levels of Cu, K, Ni, and Sr, marking the group as distinct from the others. The authors suggest that the elevated Pb levels in the Edo bones were related to environmental pollution caused by human activity.

Hrdlicka et al. (2010) used LIBS and LIBS-ICP-MS to analyze bone samples as well as organic tissue. One of the issues they ran into was a loss of data collected from the porous spongy material on the inside of the bone. The researchers knew the amount of several minor and major elements present in the sample of bone (a tibia shaft), so they recognized the lower elemental content present in the spongy bone. In the results and discussion, they reported that sections of transverse compact bone provided a well-defined distribution of both major and minor elements. Furthermore, a sample of the tibia was embedded with epoxy resin and polished to minimize the matrix effect. However, it was questioned as to whether the epoxy resin skewed the average ablation rate. It is possible that the epoxy created different excitation conditions in the microplasma above the real bone sample, suggesting ablation of bare bone surfaces is the preferred method.

Golovanova et al. (2011) designed a study similar to Brätter et al. (1977) using atomic emission spectral analysis to determine the elemental composition of human bone tissue. The elements Ca, P, Mg, Fe, Mn, Al, Si, Ti, and Sr were the focus of the study because of their role in bone metabolism. The results showed similar elemental content in bone tissues to previous literature, and they confirmed the findings of Brätter et al. that elemental composition is related

to the specific type of bone, as well as the pathological processes taking place in the bones. Their samples included bones from arthritic individuals which showed further variations in Ca and P content within hydroxyapatite, specifically higher concentrations of Ca and lower concentrations of P, suggesting a connection to metabolic processes. Furthermore, samples with arthritis had twice as much Fe compared to the non-arthritic group, and an accumulation of Fe in the bony matrix can lead to structural and mechanical changes in the bone.

János et al. (2011) performed multielemental analysis of human bone samples from two 10^{th} century AD Northeastern Hungarian cemeteries. XRF was used to determine elemental compositions of bones and to understand whether the burial environment impacted the elemental content of the remains. Lumbar vertebral bodies from two individuals were analyzed using energy-dispersive polarization X-ray fluorescence (EDPXRF) to quantify the levels of P, Ca, K, Na, Mg, Al, Cl, Mn, Fe, Zn, Br, and Sr. The results indicated that the burial environments increased the levels of Fe and Mn in the bone, as can be expected via mineral exchanges during diagenetic alteration processes. The authors concluded that Zn, Sr, and Br were more likely accumulated during life through dietary habits. Despite being from different cemeteries with varying burial environments, the two individuals under examination could not be distinguished from each other using this method.

Mazalan et al. (2018) employed LIBS to determine the Ca/P ratio of hydroxyapatite in animal bones. Hydroxyapatite is an important compound in medicine because it is used to create bone cement. In order for the bone cement to be compatible with a patient's bones, the Ca/P ratios in the hydroxyapatite must match, allowing the broken bone to bond with the bone cement to repair the broken bone. In this study lamb, bovine, and fish bones were prepared by boiling, drying, crushing, and palletizing them into pellets of identical mass. Once the samples were

analyzed by LIBS, the spectral data were examined for the Ca I and P peaks at 442.54 nm and 534.59 nm, respectively. Using these peaks, the Ca/P ratios were calculated for each species and the amounts were verified by EDX. The results showed that LIBS provides an accurate method for measuring the Ca/P ratio in bones.

Cremated/Burned Remains

Piga et al. (2008) studied the application of X-ray diffraction (XRD) analysis to extract information from burned bone. The ability to determine the temperature and duration of a fire would greatly benefit forensic investigations since burning causes significant changes to the skeleton. Piga et al. burned 57 human bone sections and 12 molar teeth at varying temperatures between 200 and 1000ºC while noting the effects of burning at 0, 18, 36, and 60 minutes. When subjected to high temperatures, the crystalline structures within hydroxyapatite become larger, with higher temperatures generally resulting in larger crystal structures. The results determined that the growth of these crystals is directly related to the applied temperature, which can be calculated using a nonlinear logistic equation. The authors conclude that XRD analysis can provide the forensic investigator with useful information about burned skeletal remains including an estimate of time exposed to fire.

Gallello et al. (2013) set out to reconstruct the biological mineral content of Iberian skeletal cremains using inductively coupled plasma optical emission spectroscopy (ICP-OES). ICP-OES determined the biomineral content of the skeletal cremains and further statistical methods were applied to the data. Principal Component Analysis revealed the elemental profiles of bone and soil samples were different, however outer portions of the bones appeared more similar to the soil than the inner portions. Partial least squares discriminant analysis was used to

classify the bone samples based on stages of degradation. The PLS-DA results confirmed that carbonized bones can be distinguished from cremated bones, suggesting further classification of bone samples subjected to unknown thermal conditions may be possible using their elemental composition.

Tofanelli et al. (2014) discusses the matrix effect and the problems it causes for LIBS analysis. This issue can apparently be overcome using standard-less analytical methods, such as the calibration-free LIBS approach. It is suggested in other research that the samples be compacted into pellets for laser ablation analysis, but that would not be the best approach for bone samples that would be needed for further analysis, and therefore should be minimally modified. The authors considered the different results from LIBS between three sample sets of bone: untreated bone, forensically cleaned bone, and burned bone. They found that the LIBS analysis remained possible after the thermal treatment of cleaned bones or bones subjected to burning. The researchers were focusing on the elements associated with diet, which were not changed by the thermal processes, but other major organic elements were influenced. However, it was determined that at least one calibration of a known element was proven useful to ensure accuracy with the LIBS analysis.

Gilpin & Christensen (2015) evaluated XRF for the purpose of detecting non-skeletal contaminants in cremains. The authors contaminated cremated skeletal poodle remains with concrete mix before analyzing 11 samples with XRF. During cremation, most of the organic components in bone are destroyed leaving only inorganic material like hydroxyapatite, which is composed mainly of minerals. Ca, P, Cu, Fe, Mn, K, and Zn are the main inorganic components found in bone, even after the skeletal material has been reduced by burning. Using linear regression as a percent of cremains, it was shown that as the proportion of skeletal material to

contaminant changed, the levels of P, K, Zn, Al, and S also changed, validating the use of XRF for identification of non-skeletal material in contaminated cremains.

In a study similar to Gallello et al. (2013), Cascant et al. (2017) employed a spectroscopy technique to study the environmental impact on burned bones. The study implemented near infrared spectroscopy (NIR) as a method of classifying 38 burned bone samples from Corral de Saus Necropolis based on their burning conditions. Being able to determine which bone samples were less burned helps investigators identify which bones could still be analyzed forensically. Like Gallello et al. (2013), PLS-DA was used to classify bone samples based on their conditions, providing an accurate method for discriminating calcined bone from carbonized bone. Furthermore, the authors were able to build a calibration model using the NIR spectra to be used for future classification of burned bone samples.

Commingled Remains

Castro et al. (2010) examine the possible application of laser ablation-inductively coupled plasma-sector field mass spectrometry (LA-ICP-SF-MS) for the purpose of discriminating individuals using elemental compositions of bone and teeth. The authors focus on the presence of trace metals in the body because of their potential for providing information about an individual's environment. Mg, Al, Mn, Fe, Cu, Zn, Rb, Sr, Ba, and Pb were chosen for discrimination purposes since they are commonly found in the inorganic matrix of bones and teeth, and some of the elements can be influenced by an individual's specific environment (i.e., Pb, Sr). LA-ICP-SF-MS analysis was performed on bones samples from 12 individuals and tooth samples from 20 individuals. Discrimination between bone samples was most accurate when the femur and humerus were considered separately, with femora providing 75.2% correct

classification. Despite full discrimination not being achieved with the bone samples, discrimination using teeth was improved when the enamel, dentine, and cementum layers were considered separately. The authors call for further studies on elemental variation within the human skeleton in order to determine which bones are best for intra- and inter-individual discrimination.

Moncayo et al. (2014) used LIBS to analyze 25 bone samples (right femur) from 5 individuals and 12 teeth samples from 4 individuals. They collected the bones from a local graveyard in Spain, under permission by the local authorities, then brushed the bones with distilled water (no soap) to remove remaining soft tissues and sediment and let them dry before analysis. Bone and teeth samples were measured directly in air at atmospheric pressure. Home-made neural network software was developed to automate the classification. Ca, Sr, and Mg (i.e., 390–410 nm, 420–480 nm, and 516–532 nm) were used because these elements are the most representative of bone composition and are strongly dependent on individual metabolism. All samples were correctly classified to the corresponding individual membership with a spectral correlation higher than 98%. The elemental composition of the bones of various individuals differed significantly, allowing their discrimination from a LIBS-based spectral measurement of their bones. The authors concluded that the selection of Ca, Mg, and Sr signals, combined with a neural network, allowed for the discrimination of individuals with high accuracy, despite the complex matrix of the bone and teeth.

Finlayson et al. (2017) provide a comparative analysis of techniques commonly used to resolve cases of commingled human remains, including one method of elemental analysis. The authors present seven different approaches to sorting the commingled and disarticulated remains of two individuals: reconstruction, articulation, visual pair-matching, osteometric pair-matching,

taphonomy, DNA analysis, and pXRF. The pXRF was used to compare variation in elemental composition between skeletal samples, specifically looking for differences between Si, P, K, Ca, Mn, Fe, and Co. Phosphorus showed the greatest discriminating potential because it had the least amount of overlap between the two skeletons. Phosphorus concentrations were then used to assign each of the skeletal elements to one of the two individuals, resolving the commingling. Compared to the six other methods of resolution, the results obtained from the pXRF were in agreement, validating the use of elemental analysis for individual discrimination.

Archaeology

Rusak et al. (2011) utilized LIBS to assess preservation quality of archaeological remains through the measurement of Ca and F ratios. LIBS data shots were taken on the surface and at varying depths of approximately 6000-year-old sheep and cattle bones. Rusak et al. chose to measure Ca/F ratios using the emission lines Ca I and F I at 671.8 nm and 685.6 nm, respectively. Ca/P ratios were not measured due to iron interferences which left most of the spectra below 650 nm unusable. Previously, the sheep and cattle bones had been analyzed for preservation quality using C/N ratios, providing Rusak et al. with a method for comparison. The study found that the Ca/F ratios started lower and continued decreasing during laser pulses into poorly preserved bone. In contrast, the Ca/F ratio was higher and increased with continued laser pulses into well-preserved bone. The ratios from the well-preserved bones were used to assign a discriminator value of 5.70 which could be used to differentiate between bones with varying degrees of preservation.

Kasem et al. (2011) studied Egyptian archaeological samples of bones to measure the influence of biological degradation and environmental effects. The authors used LIBS because of

its nondestructive nature, which is key in dealing with ancient artifacts and remains. The samples were sections of compact bone tissue from long bone shafts. This area has the highest mineral density and is less susceptible to diagenetic changes commonly found in archaeological contexts. The samples were minimally prepared: basic brushing to remove excess dirt, etc. The laser was used at wavelength 1064 nm, with a pulse duration of 5 ns in a single pulse. The pulse energy was set to 100 mJ and the repetition rate to 1 Hz. Two cleaning shots were fired, then the spectra from five consecutive shots were recorded for each spot. Kasem et al. determined that LIBS is a minimally invasive, virtually non-destructive, rapid, and portal elemental analysis technique.

López-Costas et al. (2016) examined compositional changes in archaeological human bones due to diagenesis using XRF. Thirty skeletons from the archaeological site of A Lanzada in Northwest Spain were studied to better understand the process of diagenesis and how life environmental exposure can be embodied chemically within the skeleton. Three types of bone (thoracic, long bone, and cranial) were recovered from slightly alkaline and acidic burial environments and analyzed by XRF. Principal components analysis was performed on the data allowing bone composition to be characterized by 4 chemical signals related to diagenesis of bone material, metals leaching from the soil, presence of fine silt and clay soil particles, and Pb contamination. Results showed that bones from the thoracic region were more susceptible to diagenesis and the soil environment, and the skeletons buried in the acidic soil were poorly preserved. Furthermore, the bone samples containing higher Pb concentrations were from the Roman period (as opposed to the post-Roman period). The authors hypothesize that Romans in this area may have been exposed to elevated atmospheric metal contamination.

Human vs. Non-Human

To further complicate the discrimination of bone from other materials, all positively osseous fragments must then be categorized into human and non-human. Even in the FBI's Anthropology Lab, this is typically done based on the gross shape, or morphology, of the bones (Coleman, 2013). When a fragment is not easily recognized by its morphology, histological examination under microscope may be used. According to a review of histological methods by Hillier and Bell (2007), it is also difficult to differentiate the human osteon patterns from other vertebrates, especially mammals. Moreover, this method is destructive to the sample and the histological sections require extensive sample preparation.

In *Biological Anthropology of the Human Skeleton* (Katzenberg & Grauer, 2018), Ubelaker provides an overview of anthropological methods for determining human remains from nonhuman remains, especially in cases with fragmentary or altered material. Ubelaker agrees with Hillier and Bell (2007) that microscopic analysis of small evidence allows a clearer view of the morphological details, relying on osteon organization or visual analysis of the internal structure is not always conclusive and more research should be done in this area. For cases with extremely fragmented or environmentally compromised materials, SEM/EDS may provide diagnostic results through spectral data. SEM/EDS identifies elements within a sample and the relative proportions of the elements can be used to facilitate the classification of osseous or dental materials. However, SEM/EDS will not distinguish human from nonhuman remains. For this Ubelaker recommends protein radioimmunoassay (pRIA) analysis (Ubelaker, 2004).

Vass et al. (2005) determined that cortical bone was best for the site of elemental analysis since it has less intraindividual variation than cancellous bone, and remodels in a predictable pattern throughout life. Vass et al. claim to have noted differences in the levels of Ti and Ba

present in the skeletons of European Americans and African Americans, suggesting that “This would lead to the identification of the bones based on gender, sex, and race in the case of human bones” (p. 1). Vass et al. concludes by stating that compositional differences between human and animal bones may provide an elemental fingerprint that could effectively identify fragmentary remains.

Rinke (2012) focused her dissertation on forensic analysis techniques for a variety of samples. Her work includes a section on bones from various species, including human, as well as sections about LIBS and LA-ICP-MS. She used LIBS to analyze bone samples but ran into a sampling issue when some of the samples were too large to fit into the LIBS ablation chamber. She attempted to use slivers of bone and bone dust for the analysis, but that resulted in samples that were too thin for the laser to ablate properly, so she ended up using only small bones that fit into the chamber. She used a variety of bones to test the ability to discriminate between human and non-human remains. The laser output ranged between 65- 45 mJ/pulse for the analysis, the delay after the laser pulse was between 2.5 -5 μs. Rinke tested the surface of the bone itself, without sample preparation, and the samples were not destroyed. The element represented by the first principal component was shared with 95% variance, meaning all of the bones were very similar and had to be analyzed further to discriminate between species. The results showed that LIBS discrimination could be possible, depending on further testing parameters, reduced spectral range, and a comparison between a larger number of samples. The best statistical method included nonparametric p-value distribution on the data sets.

Buddhachat et al. (2016) discusses the lack of elemental data currently available for bone, blood, and teeth of various species, as well as any cross-species comparisons of that data. The authors use handheld X-ray fluorescence, an elemental analysis method similar to LIBS, to

obtain data from horn, antler, teeth, and bone from a variety of species. It was found that the humerus was the best bone to use for species discrimination, with 80% accuracy in determining human from non-human bones. Ultimately, Buddhachat et al. state that XRF can be used as an effective tool to study elemental composition in mineralized tissue samples, and since LIBS can perform the same analyses, but arguably better when it comes to recognizing the lower organic elements, this was a good sign for the applicability of a handheld LIBS system.

Bone or not bone?

Christensen et al. (2012) aim to validate XRF for the determination of osseous or dental materials from unknown samples. When cases involve very small pieces of evidence, it is important to first determine if the sample is even skeletal in nature. XRF is a nondestructive analytical technique capable of identifying the major, minor, and trace elements in a sample. In this study, Christensen et al. analyzed a variety of materials of known origin including human bones and teeth and nonhuman bones and teeth with XRF. Other materials that appear similar to osseous fragments or that have a similar elemental composition to bone were also analyzed for comparison. For the most part, the spectra of the bone and dental samples contained distinctive levels of Ca and P and could be differentiated from the other materials in this way. These results validated the use of XRF as an effective method for determining whether unknown materials were osseous or dental in origin.

Meizel-Lambert et al. (2015) tested the use of SEM/EDX for the discrimination of osseous and non-osseous materials in combination with multivariate statistical analyses. As previously discussed, highly fragmented or taphonomically altered materials can be difficult to identify solely based on gross anatomical or morphological features. Chemical analysis

techniques can aid in this identification by providing elemental composition information, but the addition of multivariate statistical analyses allows for further discrimination of osseous and non-osseous materials with similar compositions. Sixty samples of osseous and non-osseous materials were analyzed using SEM/EDX and the data was processed using principal component analysis and linear discriminant analysis. With the outliers removed, the results showed an overall correct classification rate of 97.97%, with a 99.86% correct classification rate for osseous materials. Furthermore, an additional blind study was conducted to assess the accuracy of SEM/EDX in classifying 20 unknown samples. All of the samples in the blind study were accurately classified, further validating SEM/EDX and statistical analysis for the chemical differentiation of osseous and non-osseous materials.

Zimmerman et al. (2015) discussed several types of spectrometric analyses used in forensic contexts. LIBS was determined to be mostly beneficial to the field and can even potentially be used to differentiate between human and non-human osseous samples. Zimmerman et al. summarized that LIBS is only destructive to samples at microscopic levels, needs minimal to no sample preparation, has a rapid analysis time, and can analyze specific elemental signatures in bones that are able to differentiate between species. There is not much research being done with LIBS and bone samples, currently, so elemental concentrations have not been standardized, which makes reproducing and verifying results more difficult.

CHAPTER THREE: MATERIALS AND METHODS

Sample

Human skeletal materials were utilized from the donated skeletal collection at the Institute of Forensic and Applied Science at the University of South Florida, with permission from Dr. Erin Kimmerle, Director (see Appendix A for IFAAS Application for Research). The sample consists of 7 donors, including one set of cremains, made up of 4 females and 3 males ranging from 28 to 79 years old. Height, weight, ancestry, and medical history were self-reported by individuals prior to donation. Further details are summarized in Table 3.1. Two archaeological samples from Dr. Jonathan Bethard's medieval Transylvanian skeletal collection were analyzed for comparison between modern and historical remains. The archaeological samples included a juvenile tibia and juvenile femur, not likely from the same individual, allowing for additional comparison between contexts (modern vs. archaeological).

Table 3.1. Donor profiles.

Donor	**Age**	**Sex**	**Disposition**
D17-010	67	Female	Surface
D18-001	64	Male	Surface
D18-005	79	Male	Caged
D18-009	76	Female	Caged
D18-012	67	Male	Tarped
D18-013	73	Female	Tarped
D18-017	28	Female	Cremains

The skeletal donors were processed at the Hillsborough County Medical Examiner's Office prior to data collection. Processing of donors includes maceration in crock pots, soaking the remains in hot water with dish soap, scrubbing and brushing the bones with small brushes and wooden tools to remove remaining soft tissues, and placing the remains on trays to air dry. Further sample preparation was not required in order to perform LIBS analysis.

Data was collected at 206 locations on 29 bones across the skeleton, in order to capture the best representation of the overall elemental composition of an individual, and to test for intra-individual variation. Data was taken at 2-14 points on each skeletal element, with the number of locations dependent on bone size and morphology. Bones were selected for analysis based on size, morphology, and location in the body, with the goal of assembling a sample representative of the entire skeleton (see Figure 3.1). For example, long bones from both the left and right sides of the body were chosen, while smaller elements like metacarpals, metatarsals, phalanges, and ribs were selected from only the right side. The cranium, sacrum, and vertebrae (C2 and T10) were chosen from the midline.

To obtain the clearest spectra, the instrument's laser aperture should be flat against the sample surface to ensure the argon gas is contained in the ablation chamber and the laser ablation is consistent, minimizing noisy spectra. Examples of unusable spectra can be seen in Figures 3.2 and 3.3, the former showing a predominance of a molecular plasma (due to unfocused laser ablation) and the latter due to contamination of metallic parts in the skeleton (tooth crowns and screws). Bones with flat, smooth surfaces were preferred over curvy, convex, or concave bones due to the shape of the instrument. Locations for data acquisition were focused at or near skeletal features and landmarks instead of being randomly selected (White, 2003). However, data were still collected from as many bones and as many locations as possible (i.e., rounded distal and

proximal epiphyses of long bones), despite the morphological challenges. The cremains were analyzed by selecting fragments of bone with identifiable landmarks in order to maintain consistency within the data locations. If a bone was not recovered with the donor, that element was skipped and labeled as not available. If a specified data location was inaccessible, missing, or otherwise unable to produce clear spectra, a new data shot location was picked as close in proximity to the original spot as possible and recorded in the notes. Occasionally, the instrument was unable to access a data location due to bony protrusions, osseous formations, the angles and proximity of the surrounding bones, or fusion between skeletal elements. A complete list of skeletal elements and data collection locations can be found in Appendix B.

Tools

Data was collected using the SciAps Z-300 handheld LIBS analyzer firing a 1064 nm Nd:YAG laser at 5-6 mJ/pulse connected to the proprietary SciAps ProfileBuilder spectral analysis software (see Figures 3.4 and 3.5 on page 34). The main parameters to consider during data analysis are the power of the laser pulse used to analyze the samples, as well as the diameter of the area being analyzed (ranging from 50 to 100 μm). Each sample was analyzed at a variety of different locations (see Appendix B for complete list), with 15-25 shots taken at each point, allowing a greater amount of information to be recorded and averaged for best results.

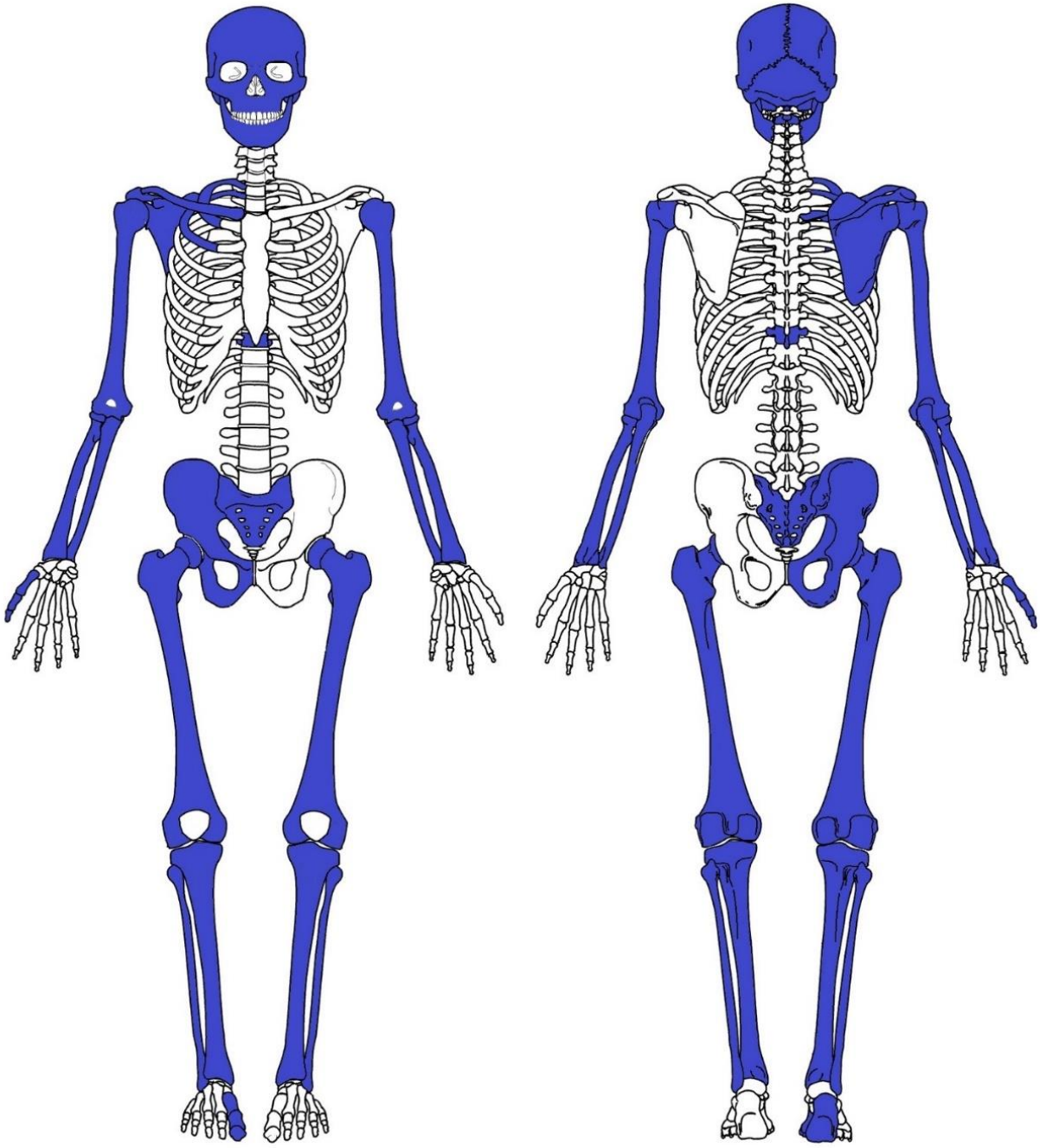

Figure 3.1. Diagram depicting the skeletal elements chosen for data collection. The bones selected for analysis are highlighted above.

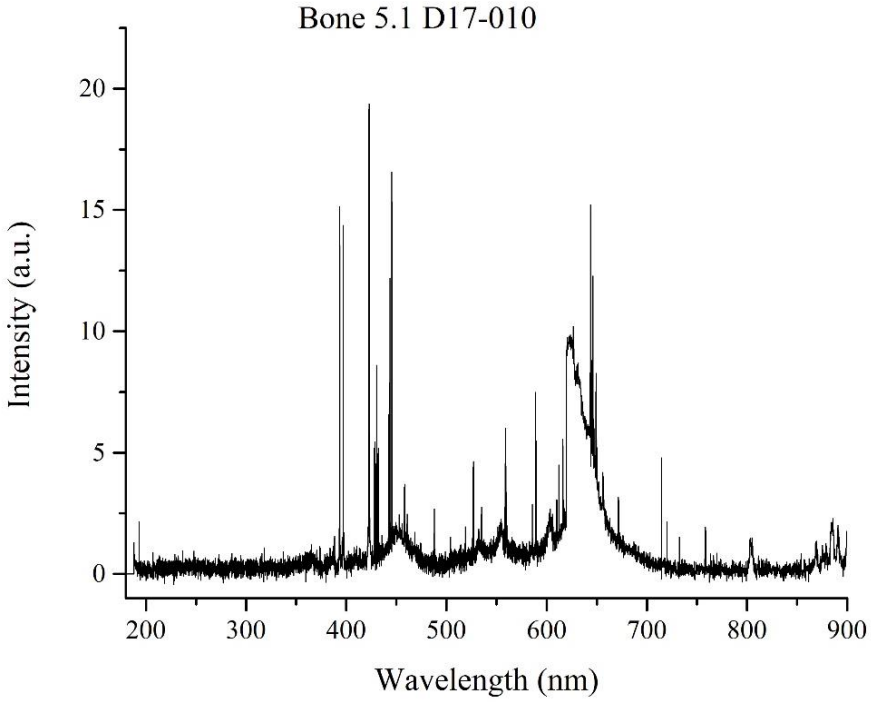

Figure 3.2. Example of a noisy spectrum obtained from the curvy, rounded radial head of the right radius from donor D17-010.

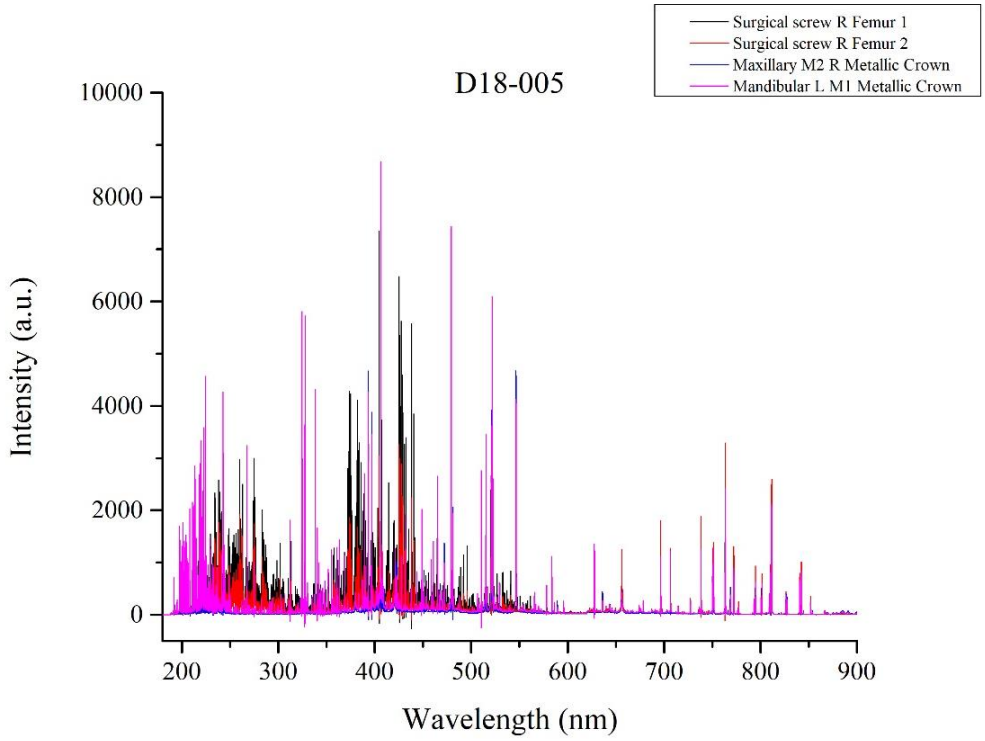

Figure 3.3. Noisy spectra obtained from metal crowns and surgical screws from donor D18-005.

Figure 3.4. SciAps Z-300 handheld LIBS analyzer used for data collection.

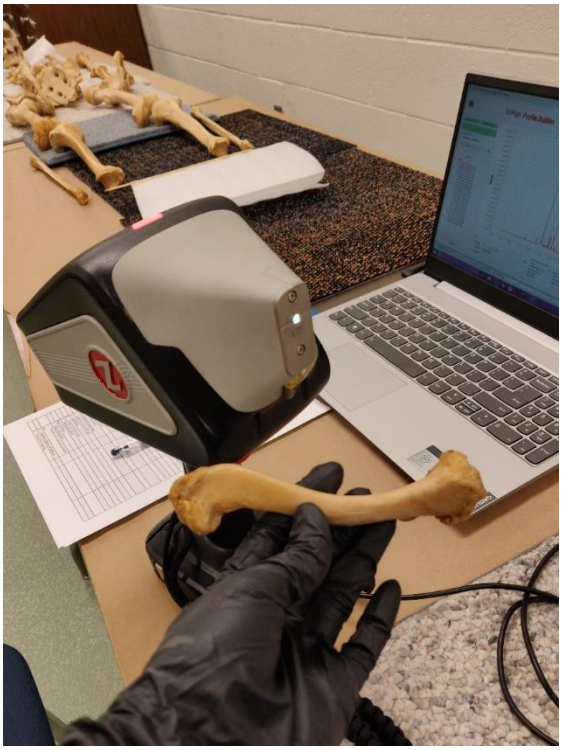

Figure 3.5. Laser aperture and analysis chamber on the front of SciAps Z-300 handheld LIBS analyzer.

Data Exploration

Prior to data analysis, the spectra at each location were visually examined for quality, consistency, and low signal to noise ratios, meaning peaks associated with the samples were easily distinguishable from background noise and excess, messy peaks. An example of clear, usable spectra is shown in Figure 3.6, and can be compared to the noisy spectra depicted in Figures 3.2 and 3.3, above. Additionally, averaged spectra for each donor is located in Appendix C. During data collection, observations were recorded for any issues encountered by the instrument associated with factors like highly porous areas, greasy bones, and locations that were too concave or convex for the instrument to obtain clear spectra. These "problem areas" were tallied across all donors in order to determine which bones and shot locations allowed for the best data collection. Furthermore, locations and bones that provided subpar spectra were excluded from some aspects of data analysis to prevent skewing results.

Additionally, the literature was consulted to determine which elements and peaks could most effectively aid in the process of discriminating between individuals. Elements and their associated spectral lines from the literature were compiled and cross-referenced with the spectra collected from the LIBS analysis, focusing on the UV-Visible spectrum ranging from wavelengths between 200-800 nm. Only the peaks present in the spectral data obtained from the donors were kept for further analysis. These peaks and their elements (70 total) are listed in Table 3.2.

Once the peaks were selected for analysis, exploratory statistics were performed using the data obtained from donor D18-005. Donor D18-005 was picked because it was the most complete skeleton and produced the best spectral data overall. The data from each shot location (204 total) on every bone selected for analysis (29 bones) were compiled into Origin Pro 9.0

(OriginPro, 2013) and normalized to the Ca peak at 370.6 nm. Using IBM SPSS Statistics 25, a box plot was produced to explore how the 70 selected peaks varied across the skeleton in one individual (IBM Corp., 2017). Results are shown in Figure 3.7. The box plot was needed to confirm that the elemental distribution did not vary too greatly within one individual, as this would make the process of differentiating separate individuals from each other more complicated, or it could prevent differentiation altogether. The box plot shows that some elements, like Ca for example, vary greatly within the skeleton at different peaks.

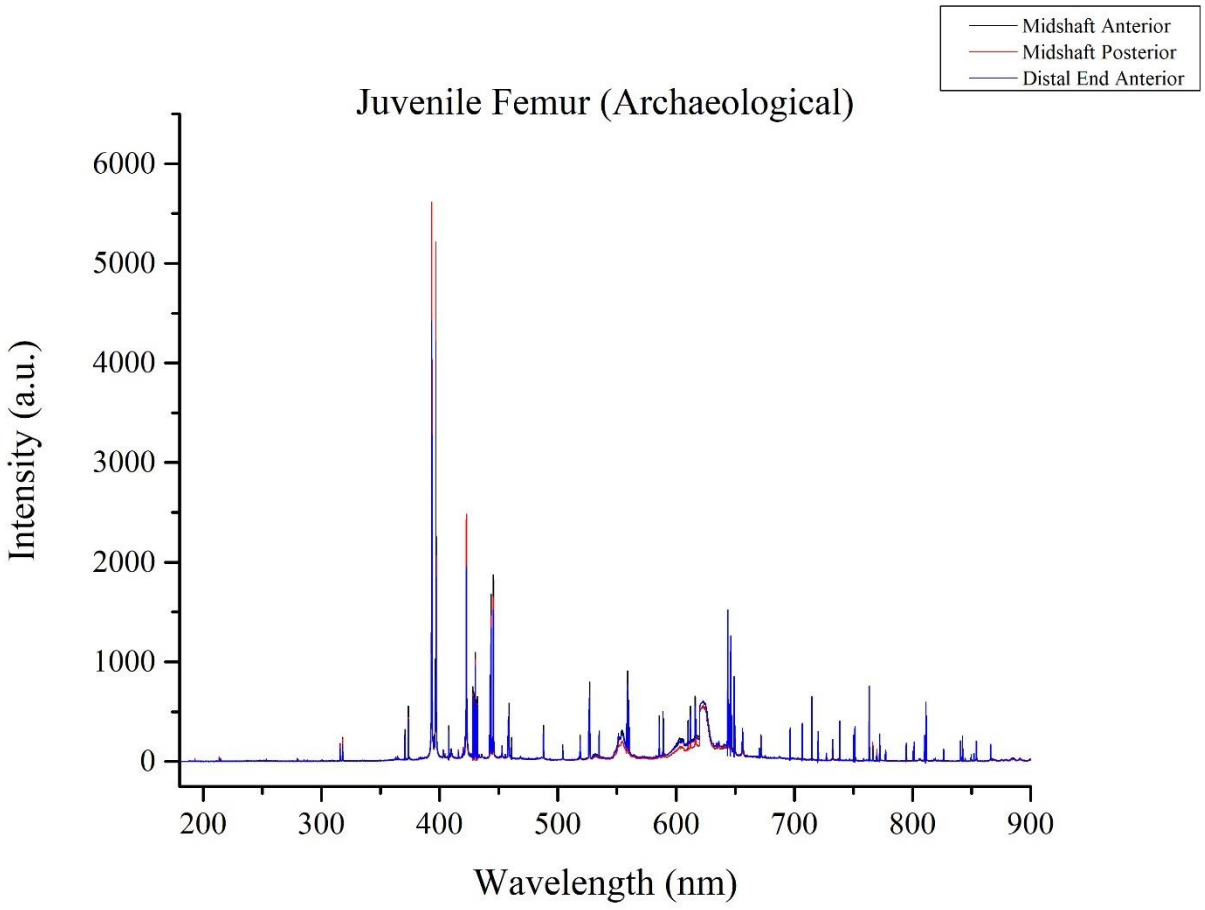

Figure 3.6. Clear spectra with a low signal-to-noise ratio obtained from 3 locations on a juvenile femur from an archaeological context.

Table 3.2. Elements used for further data analysis.

Element	Wavelength (nm)	Element	Wavelength (nm)	Element	Wavelength (nm)
Zn	206.2	Fe	360.9	Ba	493.408
Zn	213.83	Ca	370.6	Fe	495.8
P	214.93	Fe	371.993	Ca	504.8
C/Fe	247.856	Fe	373.713	Mg	517.3
Ba/Mn	257.56	Fe	374.948	Mg	518.36
Fe	259.9	Fe	375.823	P	534.59
Fe	260.667	Fe	376.719	Ca	551.3
Fe	261.133	Ca	393.366	Ca	560.13
Fe	261.767	Al	394.4	Na	588.99
Fe	262.533	Ca	396.84	Na	589.54
Fe	262.767	Sr	407.771	Ca	610.233
Fe	263.1	Ca	420.311	Ca	612.22
Ca	272.1	Ca	422.67	Ca	616.22
Mg	279.533	Ti	430.23	Zn	636.167
Mg	280.27	Ti	430.71	Ca	643.9
Mg	285.213	Ti/Ca	430.77	Ca	671.8
Si	288.15	Ca	432	Ca	714.733
Ca	300.9	Ca	442.54	Ca/F	720.2
Al	308.2	Ca	443.5	Ca	732.6
Al	309.267	Ca	445.48	K	766.49
Ca	315.89	Ca	452.69	K	769.833
Ca	317.933	Ba	455.403	O	777.42
Ti	334.9	Sr	461		
Ti	336.1	Ca	487.813		

**(Castro et al., 2010; Katzenberg & Grauer, 2018; Gallello et al., 2013; Brätter et al., 1977; Golovanova et al., 2011; Combes et al., 2016; Kendall et al., 2018; Guimarães et al., 2016; Kosugi et al., 1986; János et al., 2011; Nganvongpanit et al., 2016b; Mazalan et al., 2018; Moncayo et al., 2015; Rusak et al., 2011; Sikora et al., 2019; López-Costas et al., 2016; Finlayson et al., 2017; Perrone et al., 2014; Gilpin & Christensen, 2015; Al-Khafif & El-Banna, 2015; Kasem et al., 2011; Jantzi & Almirall, 2014; Kaiser et al., 2010.)*

In order to confirm elemental homogeneity, a multivariate analysis of variance (MANOVA) was performed to evaluate the variance in the relative intensities at 70 elemental peaks across 29 bones in a skeleton. The univariate ANOVA results were evaluated for significance levels below p=.05, meaning they were significantly different within the skeleton. Peaks falling within this range were excluded following the reasoning that the associated elements may vary too much within one individual to be used for differentiating between

multiple individuals. Using this exclusion criteria, 24 peaks were removed from the dataset. The remaining peaks and their associated elements are presented in Table 3.3.

Discriminant function analysis (DFA) was performed after MANOVA in order to see if the bones separated into groups or if they clustered together. For individual discriminatory analysis later on, DFA resulting in tightly clustered bones is more beneficial than loosely related bones that are spread out across the combined-groups plot. The homogeneity of covariance matrices was assessed using Box's test. A scatterplot of the results appears in Figure 3.8, with the first two canonical discriminant functions accounting for 51.2% of the variance. As displayed in the axes, Function 1 (explaining 28.5% of the variance, canonical $R^2 = .76$) is weighted most heavily by Zn 636.234, while Function 2 (explaining 22.7% of the variance, canonical $R^2 = .72$) depicts the variation in Ca 422.67, C 247.856, Ca 396.84, Ca 393.366, and Ca 452.69. The two functions correctly classified approximately 63.2% of the relative elemental intensities according to their corresponding bones.

The results show that the elemental variation within the bones were similar enough that they clustered together, with only bones 11 and 12 (cranium and mandible) slightly separated from the group (see Figure 3.8). DFA was performed a second time once the excluded peaks were removed from the dataset, and the resulting combined-groups plot confirmed the bones clustered into one group, with bones 11 and 12 no longer separated from the others (see Figure 3.9). A scatterplot of the results appears in Figure 3.9, with the first two canonical discriminant functions accounting for 45.5% of the variance. As displayed in the axes, Function 1 (explaining 23.5% of the variance, canonical $R^2 = .81$) is weighted most heavily by Ti 430.23, Ca 430.77, and Ca 422.67, while Function 2 (explaining 22.1% of the variance, canonical $R^2 = .80$) depicts the variation in Ca 317.933, Ca 432, and Zn 636.234. The two functions correctly classified

approximately 69.6% of the relative elemental intensities according to their corresponding bones. The single cluster of bones around their distribution centroids is important because it indicates that there are enough similarities among the bones that they could belong to a single individual.

Table 3.3. Elements remaining after exclusion criteria were applied.*

Element	Wavelength (nm)	Element	Wavelength (nm)
Zn	206.2	Al	394.4
Zn	213.8	Ca	396.84
Fe	259.9	Sr	407.771
Fe	260.6	Ca	420.311
Fe	261.7	Ca	422.67
Fe	262.5	Ti	430.23
Fe	262.8	Ca	430.77
Fe	263.1	Ca	432
Ca	272	Ca	442.54
Si	288.15	Ca	443.5
Ca	301	Ca	445.48
Al	308.2	Ca	452.69
Al	309.2	Ba	455.403
Ca	317.933	Sr	461
Ti	334.9	Ca	487.813
Fe	360.9	Ba	493.408
Ca	370.6	Ca	504.8
Fe	371.993	P	534.59
Fe	373.713	Ca	560.13
Fe	374.948	Zn	636.234
Fe	375.823	K	766.49
Fe	376.719	K	769.9
Ca	393.366		

**There are multiple unique lines associated with every element caused by electrons transitioning between energy levels. The differences between energy levels determine at which wavelength the line appears in the spectrum.*

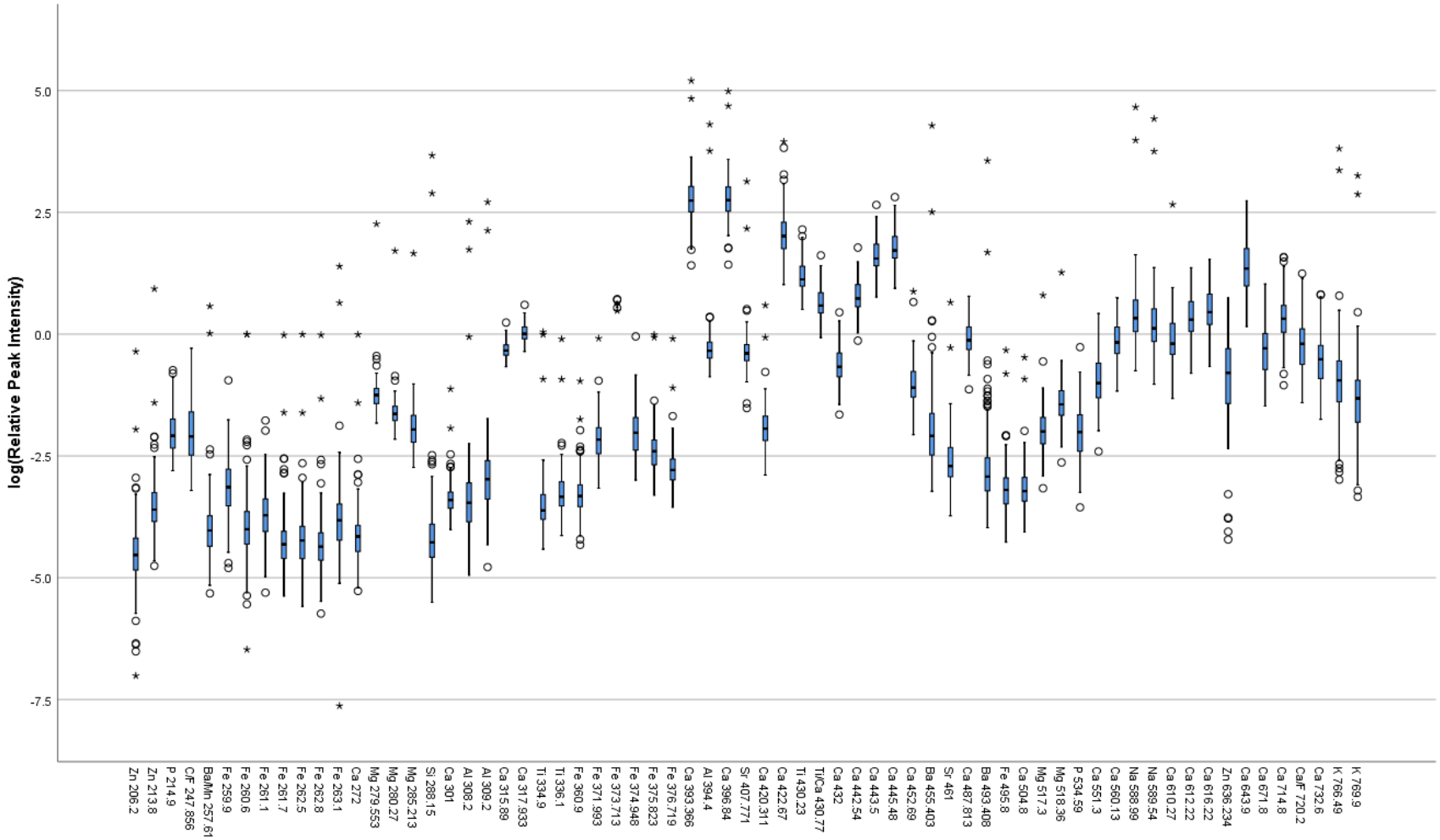

Figure 3.7. Distribution of elements across the skeleton of donor D18-005.

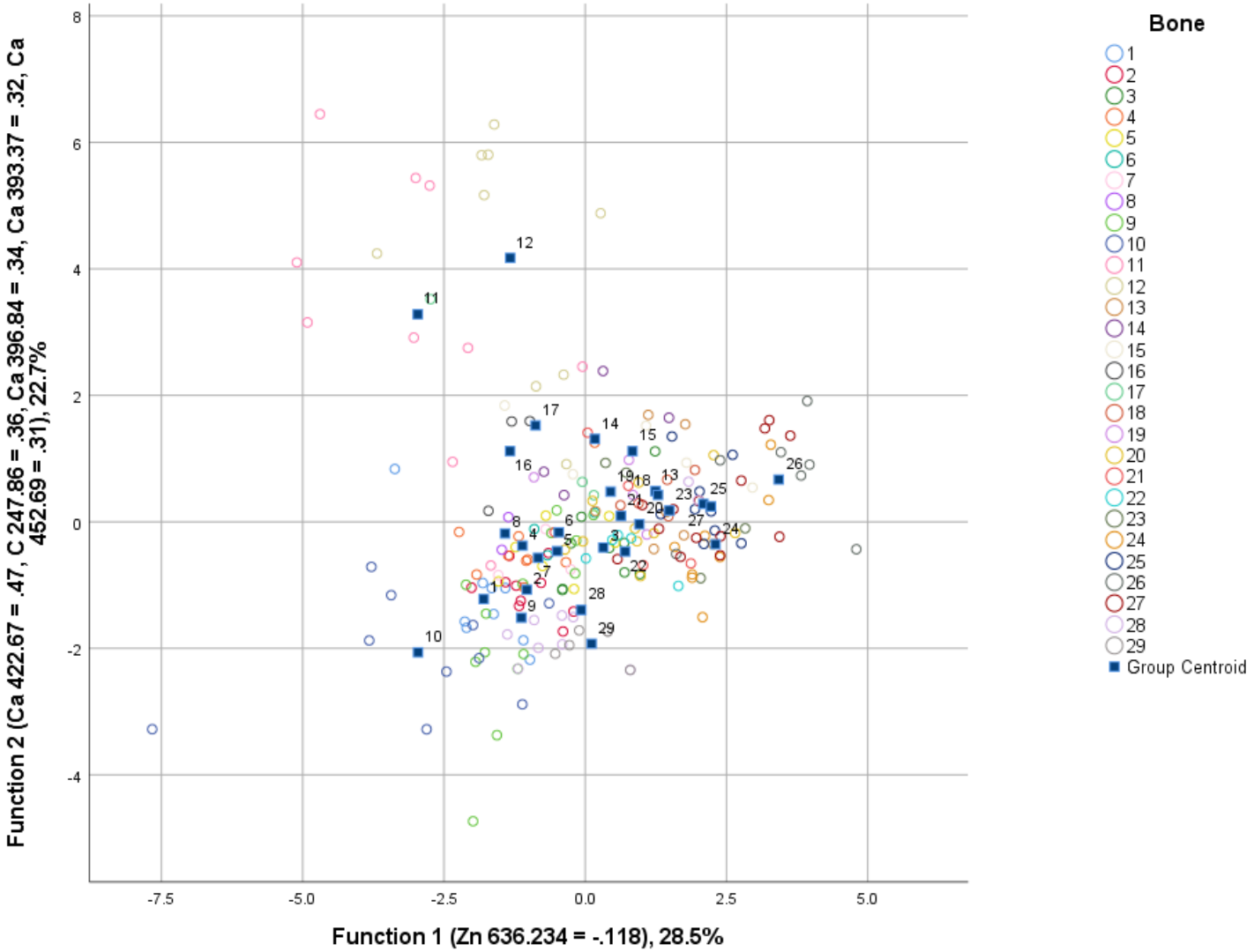

Figure 3.8. Discriminant function analysis showing clustering of bones based on elemental variation. Please refer to Appendix B for a complete list of bones.

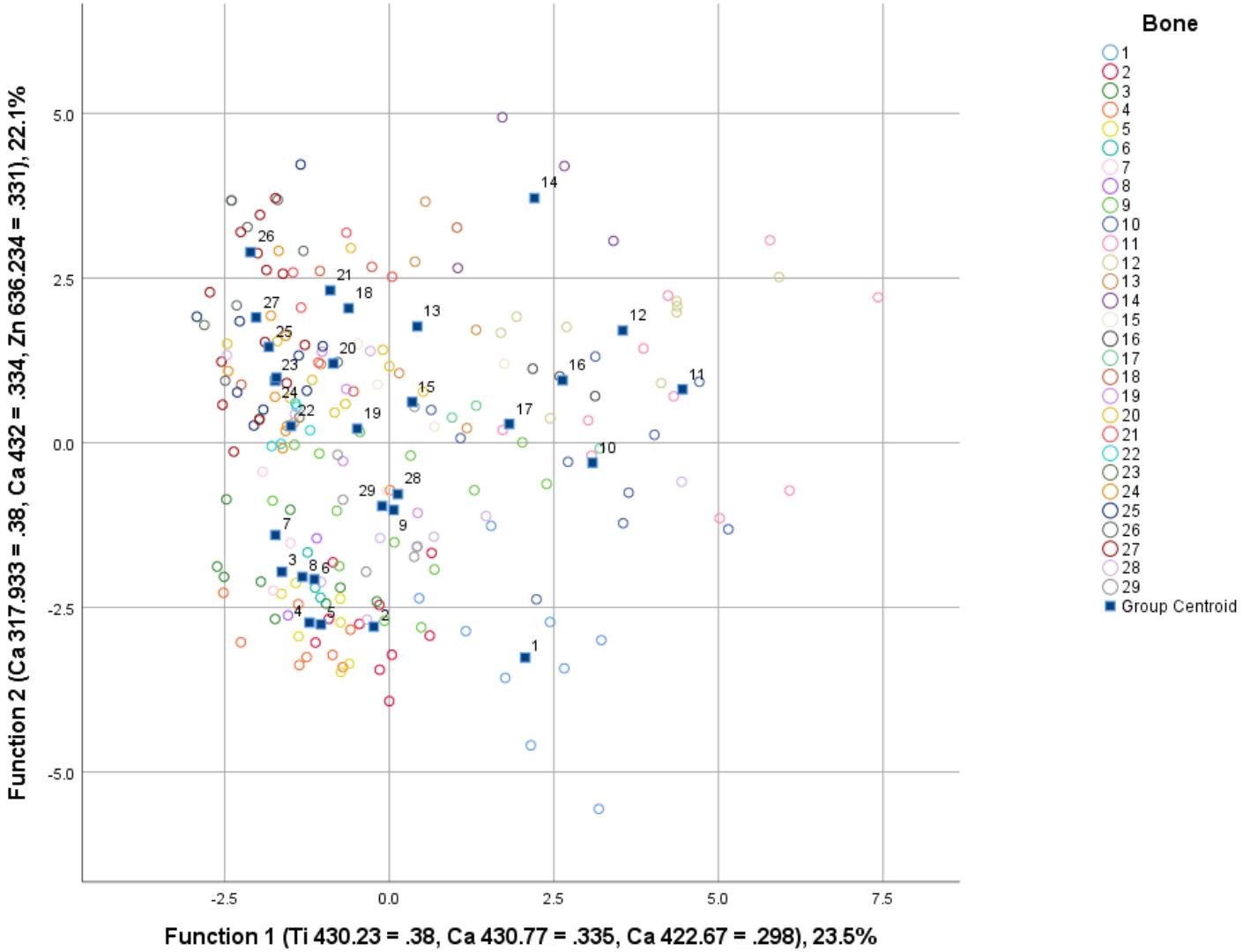

Figure 3.9. Discriminant function analysis after excluding significantly different elements from the dataset.

Statistical Analysis

After performing exploratory data analysis to understand the elemental variation across all bones within one individual, further statistical analyses were performed to test the discriminating power of LIBS between multiple individuals. First, the data was reduced to include the least problematic and most available bones and shot locations. For example, some elements of the skeleton were not recovered with a donor and marked as not available, while others were present but consistently posed problems for the instrument due to porosity, bony protrusions, fusion of elements, degradation, or curvy surfaces. Excluding these bones and locations left 28 data points to be analyzed across the skeletons of each donor. At each of these data points, the relative intensities of all 45 peaks from Table 3.3 (above) were normalized to Ca at 370.6 nm.

IBM SPSS Statistics 25 was used to perform MANOVA, post hoc analyses, and DFA (IBM Corp., 2017). MANOVA was applied to the elements at each data location to test whether each donor differs along with the elements in their bones. Post hoc analyses like Games-Howell were utilized to provide further insight into the meaning of the MANOVA test, particularly which variables contributed most to the results. DFA was employed to test the separability of groups of bones associated with each donor. Additionally, DFA was carried out on all donors to determine if burial disposition (caged, surface, tarped) could be discerned using elemental variation. Finally, an extra rib was recovered with donor D18-012 and was presumed to belong to donor D18-013. DFA was used to test this hypothesis. The results are discussed in the following chapter.

CHAPTER FOUR: RESULTS

Results from the multivariate analysis of variance (MANOVA) of elements by donor are reported in Table 4.1. Using Pillai's Trace, there was a significant effect of donor assignment on the elements present in bones: V=5.043, F(264, 906)=18.091, p<.001. In other words, the donors differ significantly with respect to a linear combination of all 45 elements selected for analysis. Separate univariate ANOVAs on the dependent variables (45 elemental peaks) found significant differences (p=.05) in all selected elements except for Ca at 301 nm (F(6, 189)=1.439, p=.202), Ti at 334.9 nm (F(6, 189)=2.773, p=.013), K at 766.49 nm (F(6, 189)=2.843, p=0.11), and K at 769.9 nm (F(6, 189)=1.831, p=.095). The Games-Howell post hoc test produced extensive results outlining the mean differences in relative elemental intensities between donors. The vast majority of the significant differences indicate that the mean differences in elements are less in the cremains (D18-017) compared to the skeletal donors.

MANOVA was followed up with discriminant analysis and considering the results of the Games-Howell post hoc test, DFA was run twice to test whether the donors could be separated into groups, first without the cremains and again including the cremains. The homogeneity of covariance matrices for all further discriminant function analyses was assessed using Box's test. A scatterplot of the results from the first test appears in Figure 4.1, with the first two canonical discriminant functions accounting for 78.7% of the variance. As displayed in the axes, Function 1 (explaining 65.9% of the variance, canonical R^2 = .97) is weighted most heavily by Ca, while Function 2 (explaining 12.8% of the variance, canonical R^2 = .87) depicts the variation in Al.

Table 4.2 displays the classification results for these two functions that correctly classified approximately 98.8% of the samples according to their respective donors.

Discriminant analysis on the dataset including the cremains revealed two discriminant functions accounting for 85% of the variance. A scatterplot of the results from the test appears in Figure 4.2. As displayed in the axes, Function 1 (explaining 61.5% of the variance, canonical R^2 = .99) is weighted most heavily by Ca 452.69 and Fe 373.713, while Function 2 (explaining 23.5% of the variance, canonical R^2 = .96) captures the variation in Ca 432. Table 4.3 displays the classification results for these two functions that correctly classified approximately 98.5% of the samples according to their corresponding donors. The discriminant function plots show that all donors can be separated into individual groups, clustered around a respective distribution centroid, regardless of the inclusion of the cremains data. Due to the significant mean difference in relative elemental intensities, the distribution centroid of the cremains is located further away from the remaining donors, which are clustered more tightly around their centroids and closer to one another.

Table 4.1. Output from multivariate analysis of variance of 45 elements by 7 donors.

Multivariate Tests[a]

Effect		Value	F	Hypothesis df	Error df	Sig.
Intercept	Pillai's Trace	1.000	10102.779[b]	44.000	146.000	.000
	Wilks' Lambda	.000	10102.779[b]	44.000	146.000	.000
	Hotelling's Trace	3044.673	10102.779[b]	44.000	146.000	.000
	Roy's Largest Root	3044.673	10102.779[b]	44.000	146.000	.000
Donor	Pillai's Trace	5.043	18.091	264.000	906.000	.000
	Wilks' Lambda	.000	30.113	264.000	877.925	.000
	Hotelling's Trace	108.539	59.340	264.000	866.000	.000
	Roy's Largest Root	66.699	228.899[c]	44.000	151.000	.000

a. Design: Intercept + Donor
b. Exact statistic
c. The statistic is an upper bound on F that yields a lower bound on the significance level.

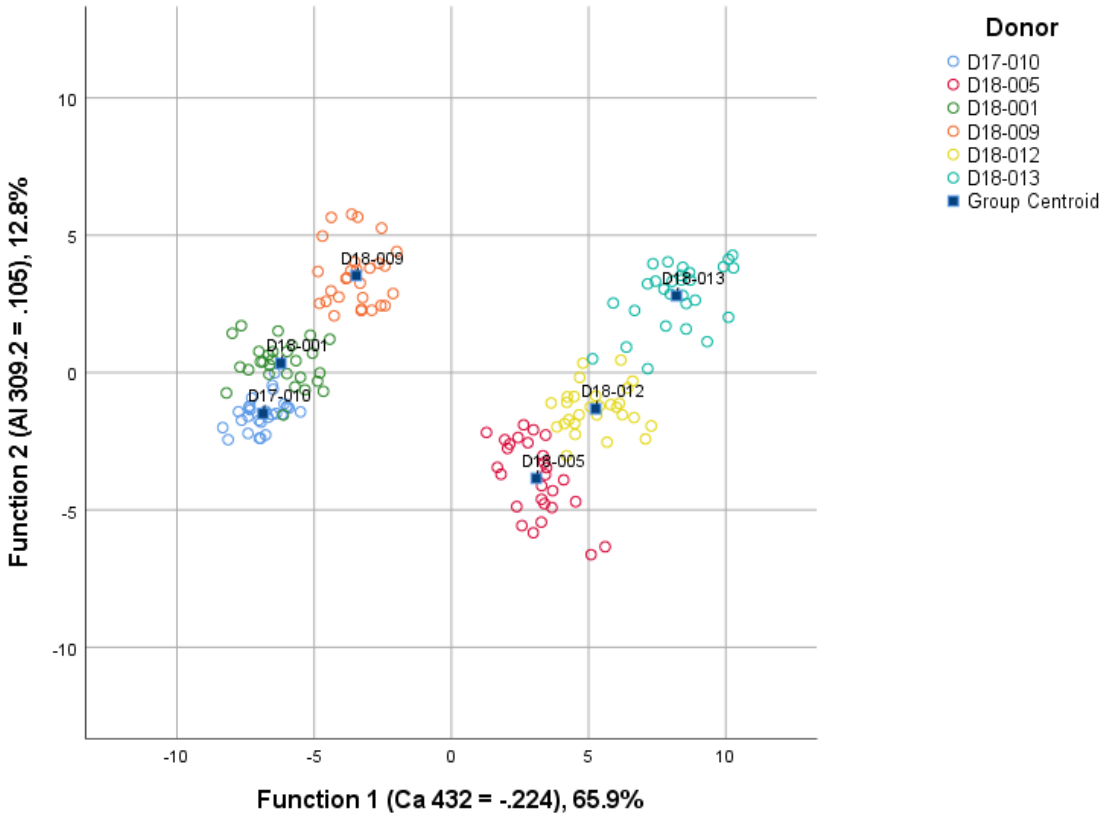

Figure 4.1. Discriminant function plot showing group separation by donor and clustering around their individual distribution centroids, cremains excluded.

Table 4.2. Classification results for discriminant function analysis, excluding cremains.

Classification Results[a]

			Predicted Group Membership						
		Donor	D17-010	D18-005	D18-001	D18-009	D18-012	D18-013	Total
Original	Count	D17-010	28	0	0	0	0	0	28
		D18-005	0	28	0	0	0	0	28
		D18-001	0	0	28	0	0	0	28
		D18-009	0	0	0	28	0	0	28
		D18-012	0	0	0	0	28	0	28
		D18-013	0	0	0	0	2	26	28
	%	D17-010	100.0	.0	.0	.0	.0	.0	100.0
		D18-005	.0	100.0	.0	.0	.0	.0	100.0
		D18-001	.0	.0	100.0	.0	.0	.0	100.0
		D18-009	.0	.0	.0	100.0	.0	.0	100.0
		D18-012	.0	.0	.0	.0	100.0	.0	100.0
		D18-013	.0	.0	.0	.0	7.1	92.9	100.0

a. 98.8% of original grouped cases correctly classified.

Table 4.3. Classification results for discriminant analysis, including cremains.

Classification Results[a]

			Predicted Group Membership							
		Donor	D17-010	D18-005	D18-001	D18-009	D18-012	D18-013	D18-017 Cremains	Total
Original	Count	D17-010	28	0	0	0	0	0	0	28
		D18-005	0	28	0	0	0	0	0	28
		D18-001	0	0	28	0	0	0	0	28
		D18-009	0	0	0	28	0	0	0	28
		D18-012	0	0	0	0	28	0	0	28
		D18-013	0	0	0	0	3	25	0	28
		D18-017 Cremains	0	0	0	0	0	0	28	28
	%	D17-010	100.0	.0	.0	.0	.0	.0	.0	100.0
		D18-005	.0	100.0	.0	.0	.0	.0	.0	100.0
		D18-001	.0	.0	100.0	.0	.0	.0	.0	100.0
		D18-009	.0	.0	.0	100.0	.0	.0	.0	100.0
		D18-012	.0	.0	.0	.0	100.0	.0	.0	100.0
		D18-013	.0	.0	.0	.0	10.7	89.3	.0	100.0
		D18-017 Cremains	.0	.0	.0	.0	.0	.0	100.0	100.0

a. 98.5% of original grouped cases correctly classified.

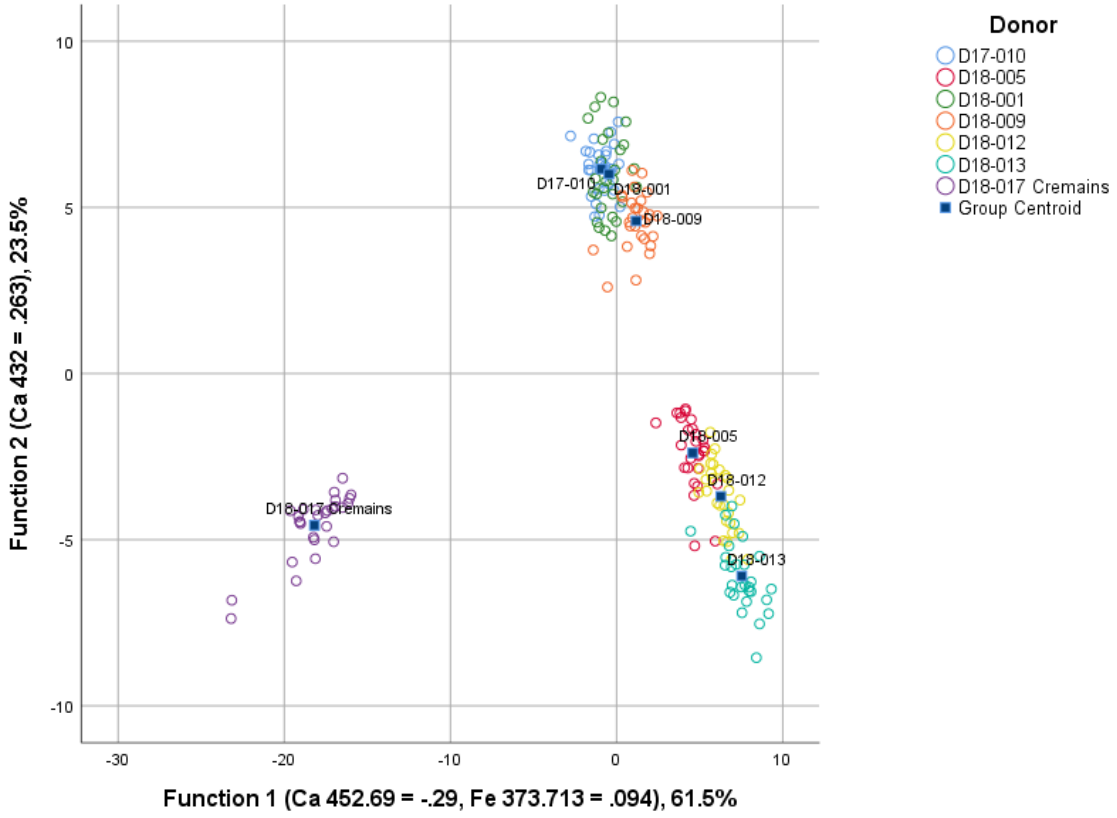

Figure 4.2. Discriminant function plot showing group separation by donor and clustering around their individual distribution centroids, cremains included.

As mentioned previously, an extra rib was recovered with D18-012 and was initially presumed to belong to D18-013 due to being placed near each other at the IFAAS Facility and having similar morphology and taphonomic profile. DFA was performed on 3 equivalent data shot locations on the extra rib and right ribs from D18-012 and D18-013 in order to test its relation to either donor. Results revealed two discriminant functions accounting for 100% of the variance. Function 1 explained 91.7% of the variance (canonical R^2 =.99) and is weighted heavily by Fe 261.7, Fe 260.6, Fe 259.9, and Zn 213.8, whereas Function 2 explained only 8.3% of the variance (canonical R^2 =.88), representing the variation in Fe 262.5 and Zn 206.2. In combination, these discriminant functions significantly differentiated the ribs, L=.001, $\chi^2(12)=22.86$, p=.029, but removing the first function indicated that the second function did not significantly differentiate the ribs, L=.120, $\chi^2(5)=7.42$, p=.191. A scatterplot of the results from the test appears in Figure 4.3. Table 4.4 displays the classification results for these two functions that correctly classified 100% of the samples based on donor affiliation. As can be seen, the extra rib does not group with either D18-012 or D18-013, suggesting the possibility of it belonging to another donor altogether.

Table 4.4. Classification results from discriminant analysis of rib samples.

Classification Results[a]

			Predicted Group Membership			
		Donor	D18-012	D18-013	Extra Rib	Total
Original	Count	D18-012	3	0	0	3
		D18-013	0	3	0	3
		Extra Rib	0	0	3	3
	%	D18-012	100.0	.0	.0	100.0
		D18-013	.0	100.0	.0	100.0
		Extra Rib	.0	.0	100.0	100.0

a. 100.0% of original grouped cases correctly classified.

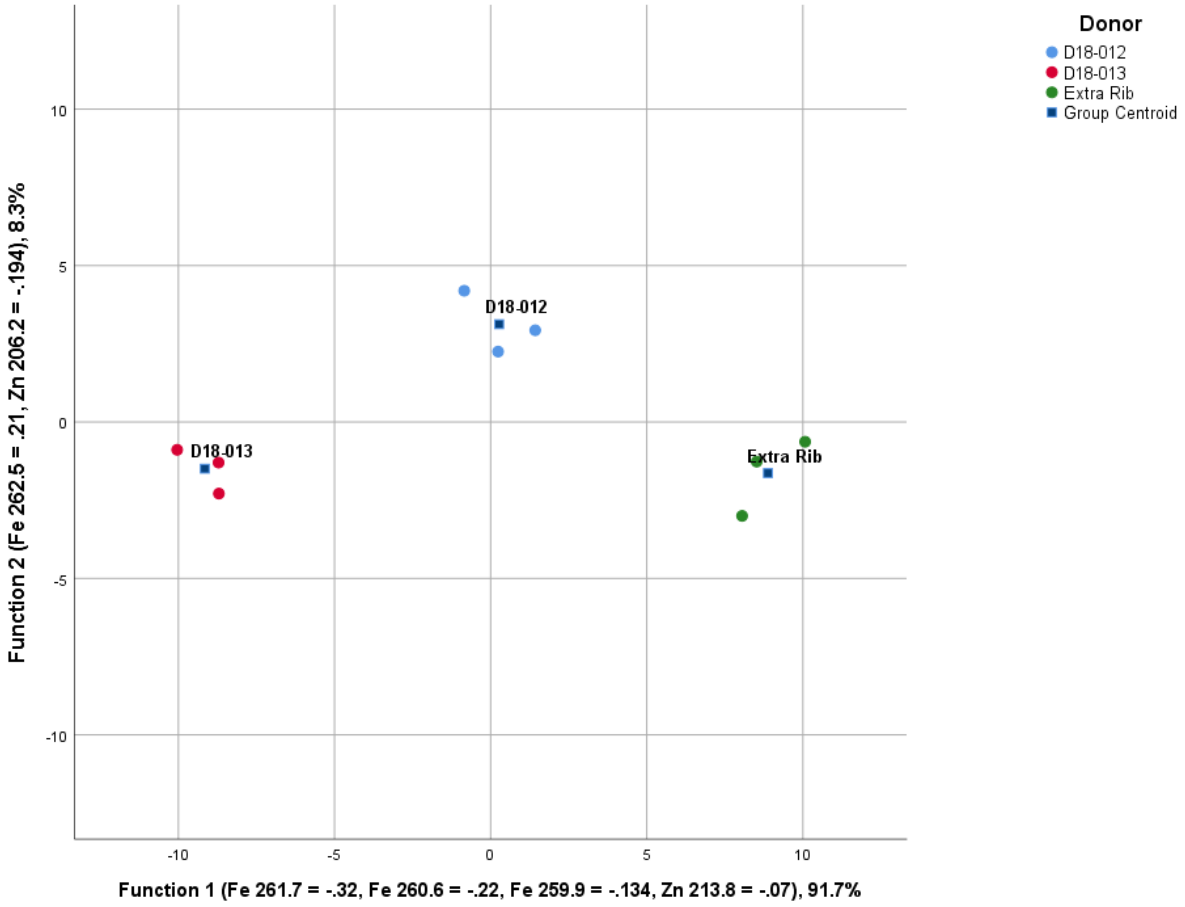

Figure 4.3. Discriminant function plot showing group separation by rib data locations and clustering around distribution centroids.

A secondary DFA was run to test whether the extra rib data would cluster with any of the donors analyzed in this project (the cremains were excluded from this analysis since the extra rib was not cremated). Discriminant analysis on the dataset including the cremains revealed two discriminant functions accounting for 78.3% of the variance. A scatterplot of the results from the test appears in Figure 4.4. As displayed in the axes, Function 1 (explaining 65.2% of the variance, canonical R^2 = .97) is weighted most heavily by Ca 432, while Function 2 (explaining 13.1% of the variance, canonical R^2 = .88) captures the variation in Sr 407.771. Table 4.5 displays the classification results for these two functions that correctly classified approximately

98.8% of the samples according to their respective donors. The secondary discriminant function plot places the extra rib closer to D18-009 than any of the other donors, but the rib could not belong to this individual. There is the possibility that using only 3 data points from each rib in the original analysis limited the discriminant functions' ability to group the extra rib with the presumed owner, but this cannot be confirmed without taking further data. Additionally, the rib was a difficult bone to obtain useful data from due to its curvy shape and surfaces. If this hypothesis were to be tested again in the future, it would be beneficial to take as many data shots along the smoother surfaces of the rib as possible in order to compile the most data for analysis.

Table 4.5. Classification results from discriminant analysis of rib samples and donors.

Classification Results[a]

			Predicted Group Membership							
		Donor	D17-010	D18-005	D18-001	D18-009	D18-012	D18-013	Extra Rib	Total
Original	Count	D17-010	28	0	0	0	0	0	0	28
		D18-005	0	28	0	0	0	0	0	28
		D18-001	0	0	28	0	0	0	0	28
		D18-009	0	0	0	28	0	0	0	28
		D18-012	0	0	0	0	28	0	0	28
		D18-013	0	0	0	0	2	26	0	28
		Extra Rib	0	0	0	0	0	0	3	3
	%	D17-010	100.0	.0	.0	.0	.0	.0	.0	100.0
		D18-005	.0	100.0	.0	.0	.0	.0	.0	100.0
		D18-001	.0	.0	100.0	.0	.0	.0	.0	100.0
		D18-009	.0	.0	.0	100.0	.0	.0	.0	100.0
		D18-012	.0	.0	.0	.0	100.0	.0	.0	100.0
		D18-013	.0	.0	.0	.0	7.1	92.9	.0	100.0
		Extra Rib	.0	.0	.0	.0	.0	.0	100.0	100.0

a. 98.8% of original grouped cases correctly classified.

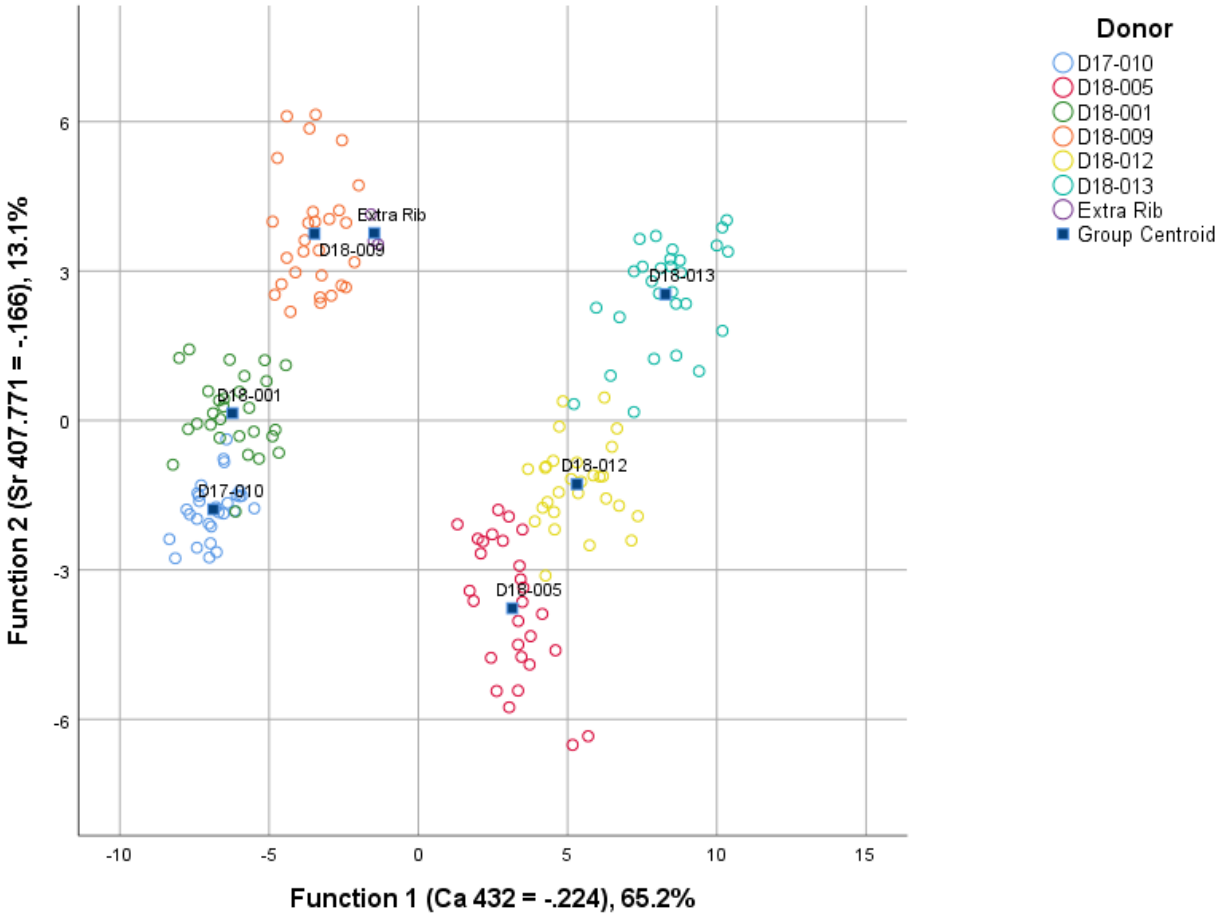

Figure 4.4. Overall discriminant function plot showing group separation by donor, including extra rib data, and clustering around individual distribution centroids, cremains excluded.

After observing the group clustering in Figures 4.1, 4.2, and 4.4, it was noted that donors D17-010, D18-001, and D18-009 clustered into a larger group separate from D18-005, D18-012, and D18-013, which formed their own larger group. Preliminary data analysis had suggested the metals from the cages had leached into the soil around the caged donors, contaminating the bones. DFA was performed to test the hypothesis that the two larger clusters were made up of donors that were placed at the IFAAS Facility under metal cages and those who were placed on the surface. DFA cannot provide a combined-groups plot for analysis between only two groups,

so the surface donors were further divided into those who were placed on the surface but also covered by a tarp.

Discriminant analysis revealed 2 discriminant functions. Function 1 explained 77.9% of the variance (canonical R^2 =.94) being weighted by 14 elements, while Function 2 explained only 22.1% (canonical R^2 =.83) and was weighted by 30 elements (see Table 4.6 for the complete structure matrix). In combination, these discriminant functions significantly differentiated the dispositions, L=.010, $\chi^2(88)=661.86$, $p<.001$, and removing the first function indicated that the second function also significantly differentiates the dispositions, L=.173, $\chi^2(43)=250.4$, $p<.001$. Table 4.7 displays the classification results for these two functions that correctly classified 100% of the samples according to disposition. The discriminant function plot is shown in Figure 4.5. Surprisingly, all 3 groups were able to be separated using the relative elemental intensities associated with bones from the respective dispositions. The data from the extra rib were included in this dataset, but the associated points do not appear to have clustered together around a distribution centroid, despite them being spread near the tarped data cluster. The results shown in Figure 4.5 indicate that individual donors can not only be differentiated from each other, but also classified by burial environment.

Table 4.6. Correlations between outcomes and the discriminant functions.

Structure Matrix

	Function			Function	
	1	2		1	2
Ca 432	-.247*	-.050	Sr 461	-.047	-.141*
Al 394.4	.116*	.059	Ca 443.5	-.006	-.127*
Al 309.2	.101*	.066	Ca 445.48	-.033	-.122*
Sr 407.771	-.100*	-.054	Ca 452.69	-.031	-.109*
Fe 374.948	.090*	.089	Ca 442.54	-.002	-.108*
P 534.59	-.074*	-.034	Ca 504.8	-.040	-.096*
Zn 636.234	-.071*	-.037	Ca 317.933	-.064	-.087*
Ca 560.13	-.064*	-.051	Ti/Ca 430.77	-.055	-.083*
Fe 375.823	.056*	.046	Al 308.2	.040	.083*
Fe 371.993	.045*	.038	Fe 360.9	.028	-.082*
Si 288.15	-.029*	.021	Ca 487.813	-.044	-.079*
Fe 376.719	.027*	-.022	K 766.49	-.005	.078*
Fe 262.5	-.024*	-.023	K 769.9	-.007	.066*
Ca 301	-.011*	-.007	Fe 261.7	-.032	-.061*
Zn 213.8	.012	.245*	Fe 259.9	.038	.061*
Ca 420.311	.101	-.225*	Ca 272	-.004	-.057*
Ca 422.67	-.014	-.177*	Pb 262.8	-.029	-.046*
Ca 393.366	.000	-.171*	Ti 334.9	-.030	-.045*
Ca 396.84	-.001	-.171*	Fe 260.6	.028	.034*
Ba 455.403	.105	-.163*	Zn 206.2	.024	.032*
Ba 493.408	.108	-.149*	Fe 263.1	.009	.023*
Ti 430.23	-.022	-.149*	Fe 373.713	.001	-.014*

Pooled within-groups correlations between discriminating variables and standardized canonical discriminant functions

Variables ordered by absolute size of correlation within function.

*. Largest absolute correlation between each variable and any discriminant function

Table 4.7. Classification results of discriminant analysis by disposition.

Classification Results[a]

			Predicted Group Membership			
		Disposition	Caged	Surface	Tarped	Total
Original	Count	Caged	56	0	0	56
		Surface	0	56	0	56
		Tarped	0	0	56	56
		Ungrouped cases	2	0	1	3
	%	Caged	100.0	.0	.0	100.0
		Surface	.0	100.0	.0	100.0
		Tarped	.0	.0	100.0	100.0
		Ungrouped cases	66.7	.0	33.3	100.0

a. 100.0% of original grouped cases correctly classified.

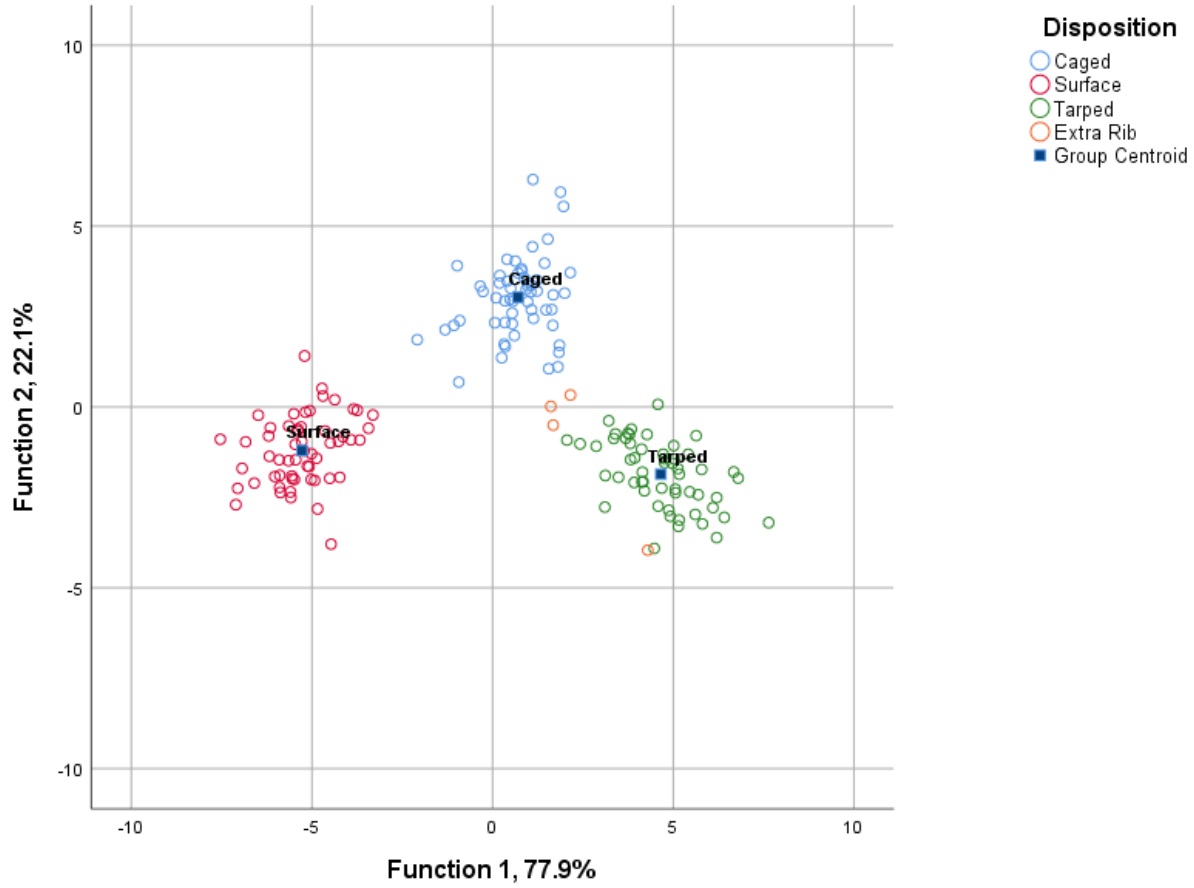

Figure 4.5. Discriminant function plot showing group separation by disposition and dense clustering around distribution centroids, extra rib data included.

The sample used for LIBS analysis included 6 human skeletal donors, 1 set of human cremated remains, and 2 juvenile archeological samples from medieval Transylvania. Originally, the juvenile samples were selected in order to test for age differences in relative elemental intensities within bones, but the gap between the age range for the skeletal donors (average age =71 years) and the juvenile bones is expansive, and the archeological remains had not been cleaned to remove dirt and have been handled without gloves by students. Essentially, there are a number of factors that could unfairly lead to the separation of the archaeological remains when compared to the donors from a modern context. Nevertheless, the archaeological data were added to the skeletal donor dataset, along with the extra rib data, in order to test the overall group separation. Discriminant analysis revealed two discriminant functions accounting for 73.3% of the variance. A scatterplot of the results from the test appears in Figure 4.6. As shown in the axes, Function 1 (explaining 61.5% of the variance, canonical R^2 = .97) is weighted most heavily by Ca 432, while Function 2 (explaining 11.9% of the variance, canonical R^2 = .88) captures the variation in Zn 213.8. Table 4.8 displays the classification results for these two functions that correctly classified approximately 98.9% of the samples according to their corresponding donors. Results from the final DFA are shown in Figure 4.6. Compared to Figure 4.4, the results appear very similar, with the additional archaeological specimens loosely clustered around their distribution centroids, near D18-001. Once again, there is the possibility that the limited number of data points acquired from the juvenile femur and tibia influenced the results of the discriminant function, and future analyses should include as much data from these smaller samples as possible, in addition to testing more archaeological samples in general.

Table 4.8. Classification results of discriminant function analysis.

Classification Results[a]

			Predicted Group Membership									
		Donor	D17-010	D18-005	D18-001	D18-009	D18-012	D18-013	Juvenile Femur	Juvenile Tibia	Extra Rib	Total
Original	Count	D17-010	28	0	0	0	0	0	0	0	0	28
		D18-005	0	28	0	0	0	0	0	0	0	28
		D18-001	0	0	28	0	0	0	0	0	0	28
		D18-009	0	0	0	28	0	0	0	0	0	28
		D18-012	0	0	0	0	28	0	0	0	0	28
		D18-013	0	0	0	0	2	26	0	0	0	28
		Juvenile Femur	0	0	0	0	0	0	3	0	0	3
		Juvenile Tibia	0	0	0	0	0	0	0	2	0	2
		Extra Rib	0	0	0	0	0	0	0	0	3	3
	%	D17-010	100.0	.0	.0	.0	.0	.0	.0	.0	.0	100.0
		D18-005	.0	100.0	.0	.0	.0	.0	.0	.0	.0	100.0
		D18-001	.0	.0	100.0	.0	.0	.0	.0	.0	.0	100.0
		D18-009	.0	.0	.0	100.0	.0	.0	.0	.0	.0	100.0
		D18-012	.0	.0	.0	.0	100.0	.0	.0	.0	.0	100.0
		D18-013	.0	.0	.0	.0	7.1	92.9	.0	.0	.0	100.0
		Juvenile Femur	.0	.0	.0	.0	.0	.0	100.0	.0	.0	100.0
		Juvenile Tibia	.0	.0	.0	.0	.0	.0	.0	100.0	.0	100.0
		Extra Rib	.0	.0	.0	.0	.0	.0	.0	.0	100.0	100.0

a. 98.9% of original grouped cases correctly classified.

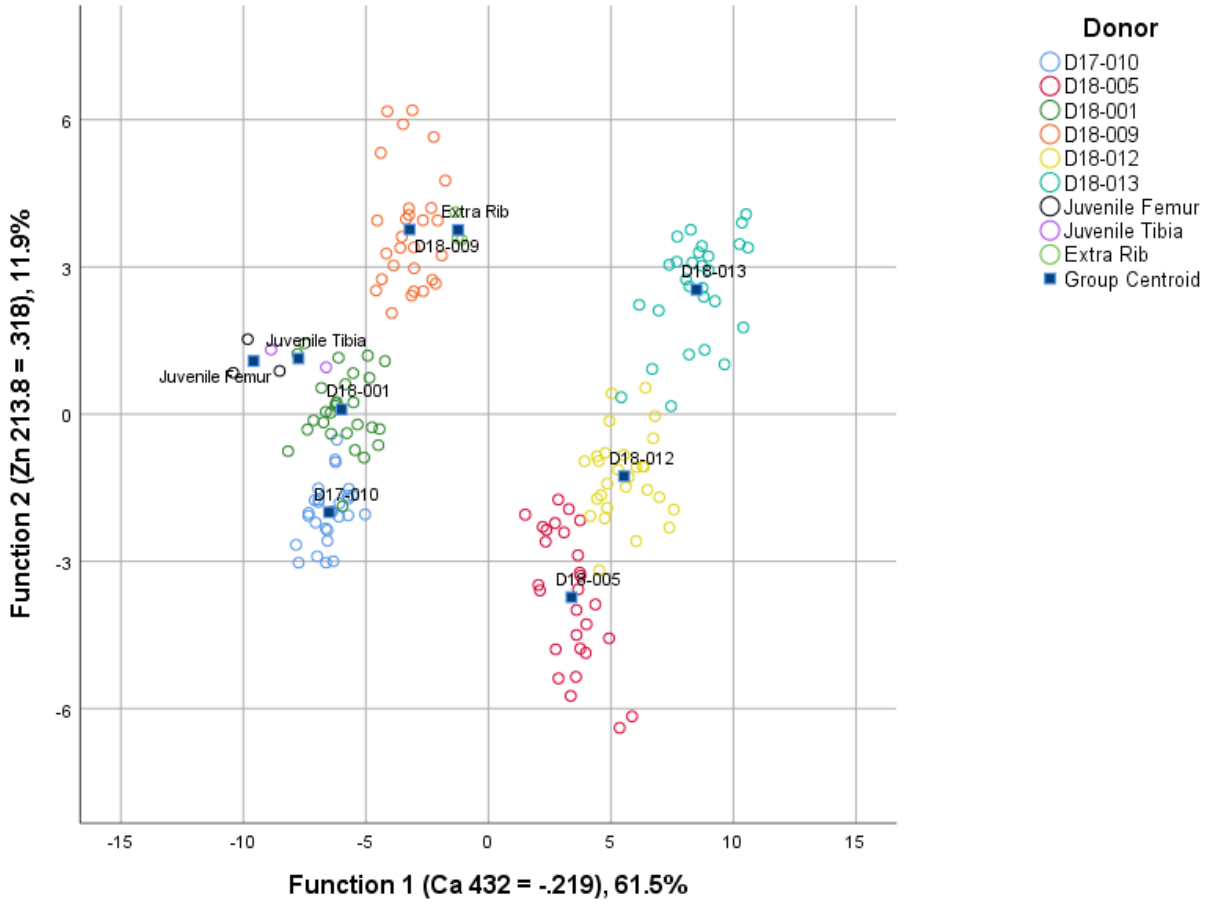

Figure 4.6. Overall discriminant function plot showing group separation by donor and loose clustering around their individual distribution centroids, extra rib data and archaeological specimens included.

CHAPTER FIVE: DISCUSSION AND CONCLUSION

Discussion

This research provides new insights into the use of Laser-Induced Breakdown Spectroscopy (LIBS) for human skeletal analysis and its ability to differentiate between individuals using elemental variation within bones. Through a combination of LIBS and multivariate data analyses, it was determined that elemental data taken from human skeletal remains could be used to differentiate each individual from another. Two questions were posed earlier in this paper: **can individuals be distinguished from one another using LIBS to obtain elemental signatures within bones? and can LIBS be considered an improvement over current methods for skeletal analysis in bioarchaeology and forensic anthropology?** The aforementioned results affirmatively answer the first question, but to resolve the second question, further discussion of the methods and results is needed.

The first analysis presented in the previous chapter revealed a significant difference between the relative elemental intensities in the donated cremains compared to the skeletal donors. The cremains spectra appeared to contain a majority of the same peaks as the other donors, so it was unlikely that the process of cremation completely removed a significant number of elements. Cremation would play a role in diagenesis, or the degradation of organic elements within bone, due to the extreme heat and thermal alteration (Gallello et al., 2013; Gilpin & Christensen, 2015; López-Costas et al., 2016; Kendall et al., 2018). However, no organic elements (i.e., O, H, C, N) were included in the list of peaks used for analysis. During data

collection, it was noted that the spectra obtained from the cremains were plotted with higher intensities than the skeletal counterparts, and the signal to noise ratios were surprisingly low. It was assumed that the chalky, ash covered bones would produce noisy spectra due to the loose materials. Seeing as this was not the case, perhaps the miniscule bone particles actually aided the instrument in detecting the elements, possibly due to increased overall surface area. During the data normalization process, it was observed that the data values were smaller than the skeletal donors, by at least one order of magnitude. In other words, there was at least one extra 0 after the decimal point before the significant figures began. This is more easily seen in the Y-axis scales of the spectral plots. For example, notice the difference between the intensity values of the normalized average spectra of the cremains (Figure 5.1) versus those of a skeletal donor (Figure 5.2). The remaining skeletal donors' averaged spectra had maximum intensities between approximately 17 a.u. and 26 a.u. (see Appendix C). This means that the separation of the cremains from the skeletal donors was more likely influenced by the instrument and the relatively higher intensities of the spectra. Something to consider in future studies may be the use of elemental ratios instead of relative peak intensities, to reduce the impact of instrumental variability and sensitivity to certain sample types.

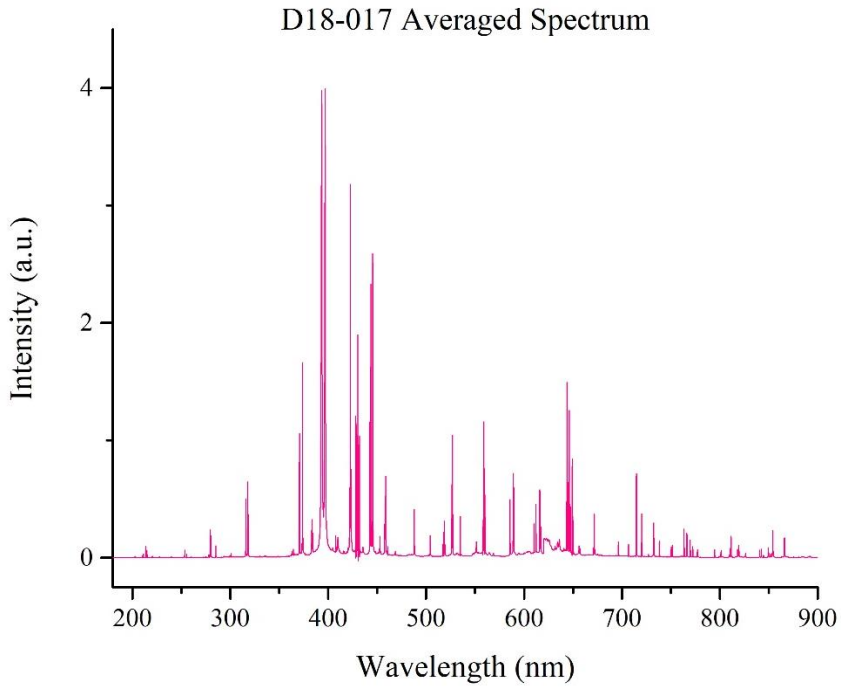

Figure 5.1. Normalized averaged spectrum from D18-017 cremains.

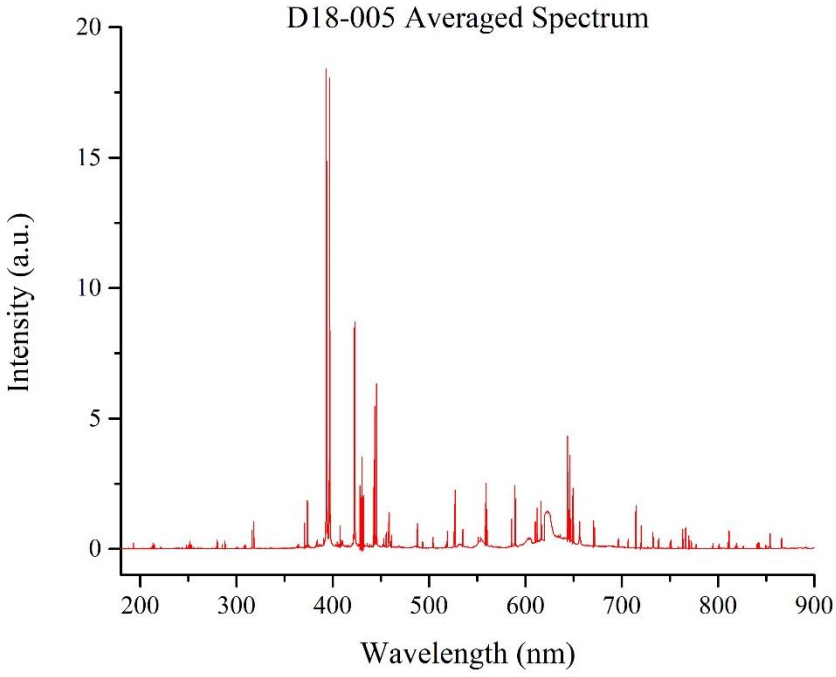

Figure 5.2. Normalized averaged spectrum from D18-005, skeletal donor.

As previously mentioned in Chapter 4, secondary clustering was observed in Figures 4.1, 4.2, and 4.4, outside of the individual donor groups. Donors D17-010, D18-001, and D18-009 (as well as the extra rib data) formed a group on one side of the discriminant function plot, while donors D18-005, D18-012, and D18-013 formed another group on the other side of the plot. This phenomenon also occurred when the cremains data were included in the analysis. Initially it was thought that the two groups were formed based on disposition, since some donors were placed under metal cages at the IFAAS Facility to prevent scavenging, while others were left on the surface or under tarps. This hypothesis was tested with a discriminant function analysis which successfully separated the donors into 3 groups based on disposition: caged, tarped, and surface, as seen in Figure 4.5. However, within the secondary groups outlined above, donors D18-005 and D18-009 were both caged but not associated within the same group. Another possibility was that they were grouped by sex, but a quick look at the donor profiles in Table 3.1 refutes this theory as well. It is possible that the two groups are defined based on the discriminant functions used in the analysis, or perhaps by variations in the LIBS instrument's analysis, but further data analysis is needed to determine which factors played a role in this additional classification.

A small-scale case of commingling was attempted to be resolved during this project. An extra rib was recovered with donor D18-012 as a result of scavenging. Due to the proximity of placement and similar taphonomic profile, the rib was presumed to belong to donor D18-013. DFA was performed on data from ribs belonging to D18-012 and D18-013 in an attempt to find its owner. As shown in Figure 4.3, the extra rib was not grouped with either of the donors. A further test was run to compare the extra rib to all of the analyzed donors (except for the cremains, since the rib was not cremated), with the resulting discriminant function plot placing the extra rib near D18-009. Unfortunately, the rib cannot belong to this donor because D18-009

was placed under a cage to prevent scavenging, and the morphology and taphonomy of the skeleton do not match that of the rib. There are other possibilities as to why the rib was unable to be grouped with a donor. First, the rib could belong to another donor that was not analyzed for this project. Second, the amount of data obtained from the single rib was not enough to confirm it belonged to D18-013. In either instance, further data collection and analysis would be required.

Limitations

Despite the promising end result, using LIBS as a means to differentiate between individuals through elemental composition came with challenges. The utilization of LIBS within bioarchaeology and forensic anthropology is still a novel concept, and the literature is lacking in clear methodologies. Moreover, techniques and procedures vary by instrument, and handheld LIBS is markedly different from a full desktop unit. Analyzing human skeletal material can be a complicated process in its own way, especially when the samples are fragmented, unrecognizable, or commingled. The following section discusses the limitations of performing skeletal analysis using a portable LIBS analyzer.

To begin, the list of elements and peaks used for analysis was compiled through an extensive review of the literature. This means that the peaks utilized for analysis were not specifically chosen from the spectra acquired from the donor sample, but instead were collected from external sources and compared to the peaks present in the sample data. Choosing to complete the analysis using sample-specific peaks could have increased the discriminating power of the tests but would have significantly increased the amount of data being analyzed (there can be hundreds of elemental peaks present in a single spectrum). Ultimately, the 45 peaks chosen for analysis were capable of discriminating individuals from one another, thus confirming the

original hypothesis. Future studies may benefit from analyzing which of the 45 peaks were most meaningful for successful discrimination, which could reduce the amount of data needed to be analyzed. Furthermore, using a peak identification utility to analyze spectral data could be beneficial to selecting elements for analysis, and the greater variety of elements may provide further insight into which are most useful in differentiating between individuals.

One of the biggest limitations of analyzing bones with the handheld LIBS instrument was the shape and size of the bones. In order to obtain the best data, the instrument's laser aperture should be pressed against the sample's surface so that the argon gas stays inside the analytical chamber, reducing interference from the outside environment. This method works with flat, smooth samples like metal and glass, but bones are rarely flat and are more likely to be porous, round, or concave. Some bones like the femur, humerus, or tibia were large and straight enough that flatter surfaces on the shafts could be used to acquire usable data. Most other bones were difficult to obtain data from because they were too small, curvy, concave, convex, rounded, fused to other elements, or susceptible to the formation of bony growths and protrusions (especially in older populations like the sample for this project). Furthermore, using a skeletal sample from a donor collection meant that some elements of the skeleton were still greasy from the decomposition process, which made it difficult for the instrument to collect clear spectra from the bones. The only way to remedy this issue is to let the bones dry more, preferably in the sun. Waiting for this process to occur can eat into valuable analysis time.

Additional limitations pertain more specifically to the LIBS system used during the analysis. The particular SciAps Z300 instrument was prone to overheating, and would fail to collect data in these situations, even after taking all of the shots required for analysis. This became a prominent issue when data was trying to be collected quickly. The time spent retaking

data shots over and over ultimately led to fewer donors being sampled than originally planned. Similarly, the instrument would interrupt data collection to recalibrate itself, a process which sometimes took several minutes to work properly.

Beyond software bugs, the instrument was physically limited by the length of the cord it required to connect to a computer, so samples had to be brought to the instrument and repositioned manually for every data shot. It is worth noting that the instrument allows data transfer through other means, but the direct connection to a computer and its proprietary analytical software was more efficient and allowed for preliminary analysis of the spectra. On the other hand, the analytical software could not be used if the instrument was not plugged in to the computer, so data analysis was also limited in that regard. The front "nose" of the instrument where the laser aperture and analytical chamber are located, was simply too long and wide to effectively maneuver around bony irregularities. If the front attachment narrowed to the size of the laser aperture, analysis of bones and other non-flat objects would be much more precise and efficient.

Further, the length of time spent analyzing samples was determined by the battery and the argon canister. The battery generally lasted between 4-6 hours, but it took almost the same amount of time to fully recharge. Fortunately, the instrument being used came with spares. The argon canister proved more limiting in that it was difficult to tell when it would run out, and then suddenly it did. This length of time varied depending on how much data was being collected, and how close to the sample the laser aperture was able to be. In the cases mentioned above when the instrument would take data shots but not save the spectra, the argon was wasted and tended to run out more quickly. The process of changing out the canisters could also be improved, since the position of the canister port inside of the instrument's handle made it difficult to screw in

without losing argon in the process. Once the argon was replaced, the instrument needed to be recalibrated, which, once again, could take several minutes to complete. For the most part, these limitations are specifically related to this instrument and its software. During the data collection process, these issues were reported to the manufacturer, SciAps. Most of the problems associated with the instrument could be resolved with software updates or by finding a LIBS system with a different physical design.

Even with the limitations discovered throughout the project, LIBS successfully analyzed more human skeletal remains than in any previous study, contributing valuable information to the literature. For future studies, it is now known which bones and locations to avoid in order to save time and reduce the amount of data to sort through during analysis. In cases with very few skeletal elements present, LIBS would offer arguably the fastest in situ data collection method, with the option to begin analysis on site as well. In order to be considered a valid method of analysis for skeletal remains in bioarchaeology and forensic anthropology, LIBS needed to be rapid, non-destructive, relatively cheap, and capable of discriminating between individuals in cases when traditional osteological analyses were not viable. The results of this study confirmed LIBS fits these criteria for elemental analysis within applied anthropology.

Implications for Applied Anthropology

As previously discussed, anthropologists utilize a variety of high-tech instrumentation to aid in the identification of human osseous material. Some of the most commonly used non-destructive techniques include XRF, SEM/EDS, LA-ICP-MS, and FTIR. These methods are useful in many situations but may not be the best choice when it comes to analyzing human skeletal remains for discrimination purposes. Comparatively, LIBS offers an easy to use

technique for rapid, non-destructive elemental analysis at a low cost and without the need for sample preparation. Of the non-destructive techniques mentioned above, LIBS and XRF offer portable or handheld versions for use in the field, making them great options for bioarchaeologists and forensic anthropologists who may not always have access to a lab.

LIBS and XRF work by analyzing elements in a sample, breaking down materials to their most fundamental level. Their non-destructive nature means they can be used on sensitive samples like evidence in a case or an ancient artifact without causing any damage. However, XRF has a few limitations when it comes to analyzing organic materials, like bone, for example. XRF is not able to detect lighter elements (low atomic mass) like H, B, and C without completing analysis in a vacuum. LIBS has high sensitivity to all elements across the periodic table, and because it uses a laser attached to fiber optics instead of X-rays, there is no risk of radiation.

Within biological anthropology, LIBS has now proven its ability to quickly, safely, and non-destructively analyze human skeletal remains in order to differentiate individuals from each other at an elemental level. This method has the potential to resolve cases of commingling more efficiently, saving time and energy during the process. In addition, very little needs to be known about who the bones belonged to in order to classify the skeletal elements together. This technique changes the way forensic anthropologists and bioarchaeologists categorize people because it develops an individual profile using elements instead of meaningless characteristics like sex and ancestry. Elemental analysis in anthropology can be used to get to the root of what individual identity really means. Beyond this, LIBS provides the gateway to a greater understanding of human variation beginning at the most fundamental level.

Conclusion

The aim of this study was to evaluate the application of Laser-Induced Breakdown Spectroscopy for use in bioarchaeology and forensic anthropology with the purpose of individual discrimination through elemental analysis. Spectral data were collected from donated human skeletal remains and two archaeological samples using LIBS. Statistical analyses like multivariate analysis of variance (MANOVA) and discriminant function analysis (DFA) were performed on the data to test the discriminating power of relative peak intensities obtained from LIBS. The results show that individuals can be differentiated from each other using elemental data, and burial environments can be similarly categorized. LIBS analysis on skeletal remains has its limitations but future studies can be designed to minimize these. Future studies should include further statistical analyses to better understand which factors most influence discrimination, how few elements are needed per individual to provide accurate discrimination, and to test for age and sex differences in trace elements.

REFERENCES

Al-Khafif, G. D., & El-Banna, R. (2015). Reconstructing ancient Egyptian diet through bone elemental analysis using LIBS (Qubbet el Hawa Cemetery). *BioMed Research International, 2015*.

Almirall, J. (2017). Laser Ablation Inductively Coupled Plasma Mass Spectrometry (LA-ICP-MS) and Laser Induced Breakdown Spectroscopy (LIBS) Analyses of Paper, Inks, and Soils.

Baker, L. (2016). Biomolecular applications. *Handbook of forensic anthropology and archaeology*, 322-334.

Balatsoukas, I., Kourkoumelis, N., & Tzaphlidou, M. (2010). Auger electron spectroscopy for the determination of sex and age related Ca/P ratio at different bone sites. *Journal of Applied Physics, 108*(7). doi:10.1063/1.3490118

Blau, S., & Ubelaker, D. H. (2016). *Handbook of forensic anthropology and archaeology*: Routledge.

Boyd Jr, C. C., & Boyd, D. C. (2018). *Forensic anthropology: theoretical framework and scientific basis*: John Wiley & Sons.

Brätter, P., Gawlik, D., Lausch, J., & Rösick, U. (1977). On the distribution of trace elements in human skeletons. *Journal of Radioanalytical Chemistry, 37*(1), 393-403.

Buddhachat, K., Klinhom, S., Siengdee, P., Brown, J. L., Nomsiri, R., Kaewmong, P., . . . Nganvongpanit, K. (2016). Elemental Analysis of Bone, Teeth, Horn and Antler in Different Animal Species Using Non-Invasive Handheld X-Ray Fluorescence. *PloS one, 11*(5).

Byrd, J. E., & Adams, B. J. (2016). Analysis of commingled human remains. In *Handbook of forensic anthropology and archaeology* (pp. 268-284): Routledge.

Cabo, L. L., Brewster, C. P., & Luengo Azpiazu, J. (2012). Sexual dimorphism: interpreting sex markers. *A companion to forensic anthropology, 10*, 248.

Cascant, M. M., Rubio, S., Gallello, G., Pastor, A., Garrigues, S., & De la Guardia, M. (2017). Burned bones forensic investigations employing near infrared spectroscopy. *Vibrational Spectroscopy, 90*, 21-30.

Castro, W., Hoogewerff, J., Latkoczy, C., & Almirall, J. R. (2010). Application of laser ablation (LA-ICP-SF-MS) for the elemental analysis of bone and teeth samples for discrimination purposes. *Forensic Science International, 195*(1-3), 17-27. doi:10.1016/j.forsciint.2009.10.029

Christensen, A. M., Smith, M. A., & Thomas, R. M. (2012). Validation of X-ray fluorescence spectrometry for determining osseous or dental origin of unknown material. *Journal of forensic sciences, 57*(1), 47-51.

Coleman, J. (2013). FBI Handbook of Forensic Services. In U. S. F. B. o. Investigation (Ed.).

Combes, C., Cazalbou, S., & Rey, C. (2016). Apatite biominerals. *Minerals, 6*(2), 34.

Dirkmaat, D. C., & Cabo, L. L. (2015). Anthropology: Embracing the New Paradigm. *A companion to forensic anthropology*, 424.

Fakiha, B. (2019). Technology in Forensic Science. *The Open Access Journal of Science and Technology, 7*(1), 1-10.

Finlayson, J. E., Bartelink, E. J., Perrone, A., & Dalton, K. (2017). Multimethod Resolution of a Small-Scale Case of Commingling. *J Forensic Sci, 62*(2), 493-497. doi:10.1111/1556-4029.13265

Gallello, G., Kuligowski, J., Pastor, A., Diez, A., & Bernabeu, J. (2013). Biological mineral content in Iberian skeletal cremains for control of diagenetic factors employing multivariate statistics. *Journal of Archaeological Science, 40*(5), 2477-2484.

Gilpin, M., & Christensen, A. M. (2015). Elemental Analysis of Variably Contaminated Cremains Using X-ray Fluorescence Spectrometry. *J Forensic Sci, 60*(4), 974-978. doi:10.1111/1556-4029.12757

Gocha, T. P., Ingvoldstad, M. E., Kolatorowicz, A., Cosgriff-Hernandez, M.-T. J., & Sciulli, P. W. (2015). Testing the applicability of six macroscopic skeletal aging techniques on a modern Southeast Asian sample. *Forensic Science International, 249*, 318. e311-318. e317.

Golovanova, O., Strunina, N., Lemesheva, S., & Baisova, B. (2011). Determination of the elemental composition of human bone tissue by atomic emission spectral analysis. *Journal of Applied Spectroscopy, 78*(1).

Gosman, J. H., & Stout, S. D. (2010). Current concepts in bone biology. *A companion to Biological Anthropology*, 465-484.

Guimarães, D., Dias, A., Carvalho, M., Carvalho, M., Santos, J., Henriques, F., . . . Pessanha, S. (2016). Quantitative determinations and imaging in different structures of buried human bones from the XVIII-XIXth centuries by energy dispersive X-ray fluorescence–Postmortem evaluation. *Talanta, 155*, 107-115.

Hark, R. R., & East, L. J. (2014). Forensic applications of LIBS. In *Laser-Induced Breakdown Spectroscopy* (pp. 377-420): Springer.

Hark, R. R., & Miller, A. L. (2014). Laser-Induced Breakdown Spectroscopy: A Closer Look at the Capabilities of LIBS, Part II. In: ADVANSTAR COMMUNICATIONS INC 131 W 1ST STREET, DULUTH, MN 55802 USA.

Hillier, M. L., & Bell, L. S. (2007). Differentiating Human Bone from Animal Bone: A Review of Histological Methods. *JFO Journal of Forensic Sciences, 52*(2), 249-263.

Houck, M. M. (2015). *Forensic chemistry*: Academic Press.

Hrdlicka, A., Prokes, L., Stankova, A., Novotny, K., Vitesnikova, A., Kanicky, V., . . . Palenikova, K. (2010). Development of a remote laser-induced breakdown spectroscopy system for investigation of calcified tissue samples. *Appl. Opt. Applied Optics, 49*(13), C16-C20.

IBM Corp. (2017). IBM SPSS Statistics for Windows (Version 25.0). Armonk, NY: IBM Corp.

János, I., Szathmáry, L., Nadas, E., Beni, A., Dinya, Z., & Mathe, E. (2011). Evaluation of elemental status of ancient human bone samples from Northeastern Hungary dated to the 10th century AD by XRF. *Nuclear Instruments and Methods in Physics Research Section B: Beam Interactions with Materials and Atoms, 269*(21), 2593-2599.

Jantzi, S. C., & Almirall, J. R. (2014). Elemental analysis of soils using laser ablation inductively coupled plasma mass spectrometry (LA-ICP-MS) and laser-induced breakdown

spectroscopy (LIBS) with multivariate discrimination: Tape mounting as an alternative to pellets for small forensic transfer specimens. *Applied Spectroscopy, 68*(9), 963-974.
Jaouen, K., Balter, V., Herrscher, E., Lamboux, A., Telouk, P., & Albarede, F. (2012). Fe and Cu stable isotopes in archeological human bones and their relationship to sex. *Am J Phys Anthropol, 148*(3), 334-340. doi:10.1002/ajpa.22053
Kaiser, J., Novotný, K., Hrdlička, A., Malina, R., Novotný, J., Prochazka, D., . . . Kučerová, P. (2010, 2010). *Utilization of selected laser-ablation-based diagnostic methods for study of elemental distribution in various solid samples*.
Kasem, M. A., Harith, M. A., & Russo, R. E. (2011). Influence of biological degradation and environmental effects on the interpretation of archeological bone samples with laser-induced breakdown spectroscopy. *J Anal At Spectrom Journal of Analytical Atomic Spectrometry, 26*(9), 1733-1739.
Katzenberg, M. A., & Grauer, A. L. (2018). *Biological anthropology of the human skeleton*: John Wiley & Sons.
Kendall, C., Eriksen, A. M. H., Kontopoulos, I., Collins, M. J., & Turner-Walker, G. (2018). Diagenesis of archaeological bone and tooth. *Palaeogeography, Palaeoclimatology, Palaeoecology, 491*, 21-37. doi:10.1016/j.palaeo.2017.11.041
Kerley, E. R. (1965). The microscopic determination of age in human bone. *American Journal of Physical Anthropology, 23*(2), 149-163.
Kosugi, H., Hanihara, K., Suzuki, T., Himeno, S.-I., Kawabe, T., Hongo, T., & Morita, M. (1986). Elemental composition of ancient Japanese bones. *Science of the total environment, 52*(1-2), 93-107.
Krishan, K., Chatterjee, P. M., Kanchan, T., Kaur, S., Baryah, N., & Singh, R. (2016). A review of sex estimation techniques during examination of skeletal remains in forensic anthropology casework. *Forensic Science International, 261*, 165. e161-165. e168.
Lambacher, N., Gerdau-Radonic, K., Bonthorne, E., & de Tarazaga Montero, F. J. V. (2016). Evaluating three methods to estimate the number of individuals from a commingled context. *Journal of Archaeological Science: Reports, 10*, 674-683.
Langley, N. R., Tersigni-Tarrant, M. A., & Taylor & Francis. (2017). *Forensic anthropology : a comprehensive introduction*. In (pp. 1 online resource (464 pages)). Retrieved from http://ezproxy.lib.usf.edu/login?url=https://www.taylorfrancis.com/books/9781315300030
Larsen, C. S. (2002). Bioarchaeology: the lives and lifestyles of past people. *Journal of Archaeological Research, 10*(2), 119-166.
Larsen, C. S. (2010). *A companion to biological anthropology* (Vol. 20): John Wiley & Sons.
LeCount, L. J., Wells, E. C., Jamison, T. R., & Mixter, D. W. (2016). Geochemical characterization of inorganic residues on plaster floors from a Maya palace complex at Actuncan, Belize. *Journal of Archaeological Science: Reports, 5*, 453-464.
Lee, R. S., Kayser, M. V., & Ali, S. Y. (2006). Calcium phosphate microcrystal deposition in the human intervertebral disc. *Journal of Anatomy, 208*(1), 13-19. doi:10.1111/j.1469-7580.2006.00504.x
López-Costas, O., Lantes-Suárez, Ó., & Cortizas, A. M. (2016). Chemical compositional changes in archaeological human bones due to diagenesis: Type of bone vs soil environment. *Journal of Archaeological Science, 67*, 43-51.
Martin, M. Z., Labbé, N., André, N., Harris, R., Ebinger, M., Wullschleger, S. D., & Vass, A. A. (2007). High resolution applications of laser-induced breakdown spectroscopy for

environmental and forensic applications. *Spectrochimica Acta Part B: Atomic Spectroscopy, 62*(12), 1426-1432. doi:10.1016/j.sab.2007.10.046
Mazalan, E., Chaudhary, K., Haider, Z., Hadi, S. F. A., & Ali, J. (2018). *Determination of calcium to phosphate elemental ratio in natural hydroxypatite using LIBS.* Paper presented at the Journal of Physics: Conference Series.
Meizel-Lambert, C. J., Schultz, J. J., & Sigman, M. E. (2015). Chemical Differentiation of Osseous and Nonosseous Materials Using Scanning Electron Microscopy-Energy-Dispersive X-Ray Spectrometry and Multivariate Statistical Analysis. *J Forensic Sci, 60*(6), 1534-1541. doi:10.1111/1556-4029.12868
Moncayo, S., Manzoor, S., Ugidos, T., Navarro-Villoslada, F., & Caceres, J. O. (2014). Discrimination of human bodies from bones and teeth remains by Laser Induced Breakdown Spectroscopy and Neural Networks. *SAB Spectrochimica Acta Part B: Atomic Spectroscopy, 101*, 21-25.
Nganvongpanit, K., Buddhachat, K., Brown, J. L., Klinhom, S., Pitakarnnop, T., & Mahakkanukrauh, P. (2016). Preliminary Study to Test the Feasibility of Sex Identification of Human (Homo sapiens) Bones Based on Differences in Elemental Profiles Determined by Handheld X-ray Fluorescence. *Biol Trace Elem Res, 173*(1), 21-29. doi:10.1007/s12011-016-0625-3
Nganvongpanit, K., Buddhachat, K., Klinhom, S., Kaewmong, P., Thitaram, C., & Mahakkanukrauh, P. (2016). Determining comparative elemental profile using handheld X-ray fluorescence in humans, elephants, dogs, and dolphins: Preliminary study for species identification. *Forensic Sci Int, 263*, 101-106. doi:10.1016/j.forsciint.2016.03.056
Origin. (2013). OriginPro (Version 9.0). Northampton, MA: OriginLab Corp.
Osterholtz, A. J., Baustian, K. M., & Martin, D. L. (2014). *Commingled and Disarticulated Human Remains*: Springer.
Perrone, A., Finlayson, J. E., Bartelink, E. J., & Dalton, K. D. (2014). Application of portable X-ray fluorescence (XRF) for sorting commingled human remains. In *Commingled Human Remains* (pp. 145-165): Elsevier.
Piga, G., Malgosa, A., Thompson, T. J. U., & Enzo, S. (2008). A new calibration of the XRD technique for the study of archaeological burned human remains. *Journal of Archaeological Science, 35*(8), 2171-2178.
Rinke-Kneapler, C., & Sigman, M. (2014). Applications of laser spectroscopy in forensic science. In *Laser Spectroscopy for Sensing* (pp. 461-495): Elsevier.
Rinke, C. N. (2012). Selective multivariate applications in forensic science.
Ross, A. H., & Kimmerle, E. (2009). Contribution of quantitative methods in forensic anthropology: a new era. *Handbook of forensic anthropology and archaeology*, 479-489.
Rusak, D. A., Marsico, R. M., & Taroli, B. L. (2011). Using laser-induced breakdown spectroscopy to assess preservation quality of archaeological bones by measurement of calcium-to-fluorine ratios. *Applied Spectroscopy, 65*(10), 1193-1196.
Samek, O., Beddows, D., Telle, H., Kaiser, J., Liška, M., Caceres, J., & Urena, A. G. (2001). Quantitative laser-induced breakdown spectroscopy analysis of calcified tissue samples. *Spectrochimica Acta Part B: Atomic Spectroscopy, 56*(6), 865-875.
Schultz, J. J. (2012). Determining the forensic significance of skeletal remains. *A Companion to Forensic Anthropology. Chichester: Wiley-Blackwell*, 66-84.
Sikora, M., Baranowska-Bosiacka, I., Rębacz-Maron, E., Olszowski, T., & Chlubek, D. (2019). The influence of the place of residence, smoking and alcohol consumption on bone

mineral content in the facial skeleton. *Journal of Trace Elements in Medicine and Biology, 51*, 115-122.
Squires, K. E., Thompson, T. J., Islam, M., & Chamberlain, A. (2011). The application of histomorphometry and Fourier Transform Infrared Spectroscopy to the analysis of early Anglo-Saxon burned bone. *Journal of Archaeological Science, 38*(9), 2399-2409.
Stewart, T. D. (1979). *Essentials of forensic anthropology: especially as developed in the United States*: Charles C. Thomas Springfield, IL.
Swaraldahab, M. A., & Christensen, A. M. (2016). The effect of time on bone fluorescence: implications for using alternate light sources to search for skeletal remains. *Journal of forensic sciences, 61*(2), 442-444.
Tica, C. I., & Martin, D. L. (2019). *Bioarchaeology of frontiers and borderlands*: University Press of Florida.
Tofanelli, M., Pardini, L., Borrini, M., Bartoli, F., Bacci, A., Dulivo, A., . . . Palleschi, V. (2014). Spectroscopic analysis of bones for forensic studies. *SAB Spectrochimica Acta Part B: Atomic Spectroscopy*, *99*, 70-75.
Ubelaker, D. (1998). The evolving role of the microscope in forensic anthropology. *Forensic osteology: advances in the identification of human remains. Springfield: Charles C. Thomas*, 514-532.
Ubelaker, D. H. (2018). Recent advances in forensic anthropology. In: Taylor & Francis.
Ubelaker, D. H., Lowenstein, J. M., & Hood, D. G. (2004). Use of solid-phase double-antibody radioimmunoassay to identify species from small skeletal fragments. *Journal of Forensic Science, 49*(5), JFS2003399-2003396.
Ubelaker, D. H., Ward, D. C., Braz, V. S., & Stewart, J. (2002). The use of SEM/EDS analysis to distinguish dental and osseus tissue from other materials. *Journal of forensic sciences, 47*(5), 940-943.
Vass, A., Madhavi, M., Synstelien, J., & Collins, K. (2005). *Elemental characterization of skeletal remains using laser-induced breakdown spectroscopy (LIBS).* Paper presented at the Proceedings of the American Academy of Forensic Sciences.
Zimmerman, H. A., Meizel-Lambert, C. J., Schultz, J. J., & Sigman, M. E. (2015). Chemical Differentiation of Osseous, Dental, and Non-skeletal Materials in Forensic Anthropology using Elemental Analysis. *Science & justice : journal of the Forensic Science Society, 55*(2), 131-138.

APPENDICES

Appendix A: IFAAS Application for Research Access

Letter of Intent

Receiving research access through the Institute of Forensic and Applied Science at the University of South Florida will allow me to begin working on my master's research project. I have been conducting research on the use of Laser-Induced Breakdown Spectroscopy in forensic anthropology under Dr. Matthieu Baudelet (UCF) since September 2015. The preliminary data supports our research's objective of using Laser-Induced Breakdown Spectroscopy to rapidly analyze the elemental variation of otherwise unidentifiable materials, in order to distinguish bone from non-bone, human bone from non-human, and individuals from one another, in a non-destructive manner. The data collected so far shows promising results for the first two parts of the project objective. Further data collection needs to be taken from a larger sample of human skeletal material to support the third part of the objective.

I already have experience working in the IFAAS lab and working with skeletal remains. I gained an enormous amount of osteological experience thanks to my current USF advisor, Dr. Jonathan Bethard, when I spent two months studying human osteology in Romania. Over those two months, I conducted independent research towards my anthropology degree, resulting in a research paper on the variety of taphonomic modifications found in the 150 skeletons I worked with over the summer. I received my anthropology BA from the University of Central Florida, where I also took forensic science and human biology courses. I met Dr. Baudelet at UCF when I joined his newly-formed research team at the National Center for Forensic Science. I spent two years working on research projects with NCFS but graduated before I was able to complete the LIBS in forensic anthropology analysis.

Now that I am an applied anthropology graduate student at the University of South Florida, I am able to ask similar questions about skeletal analysis and human identification for my thesis. My goal was to resume my LIBS research in graduate school, where I can continue to research, develop, and answer all of my applied anthropology questions. I have previously presented this research on posters at the UCF CREOL Affiliate's Day in 2016 and the 2016 Showcase of Undergraduate Research Expo. I was also selected to participate in the UCF Summer Undergraduate Research Fellowship over the summer of 2016, where I was guided through writing a manuscript on the use of LIBS in forensic anthropology. Overall, I have been intrigued by the potential use of LIBS in forensic anthropology since Dr. Baudelet first introduced it to me over three years ago, and I am more than excited to continue working with LIBS during my graduate career at USF.

Abstract

Forensic anthropology requires the classification of questionable fragmentary materials. The relatively unexplored use of Laser-Induced Breakdown Spectroscopy (LIBS) for elemental analysis in the field of anthropology is explored for rapid identification of osseous/dental fragments, as well as their identification as human or non-human.

One of the biggest challenges in the field of anthropology is the determination of human remains from non-human remains in a rapid, yet non-destructive manner. Current techniques used to identify human osseous material include histological analyses, DNA testing, and physical examinations. Unfortunately, these techniques are time-consuming, potentially destructive, and for some, can only be performed in certain conditions when larger sections of bone are easily identifiable. In cases of mass disasters, the current process of separating osseous fragments from

other materials, discriminating human remains from non-human remains, and identifying individuals from one another is simply inefficient. Laser-Induced Breakdown Spectroscopy (LIBS) can aid in the identification of human remains using rapid laser ablation to analyze elements in a sample. With this analysis occurring at the micro-scale, the technique is virtually non-destructive to the sample and cannot typically be seen by the naked eye.

The only sample collection needed is done at this micro-scale. The portable LIBS instrument will fire a 1064 nm laser at 5-6 mJ/pulse, taking data from a spot of bone 50-100 um in diameter on the surface. The analysis happens in under one second, with a firing rate of 50 Hz (50 shots fired per second). Using ratios of certain elements (calcium, potassium, magnesium, etc.), osseous/dental fragments can be separated from non-skeletal samples. Furthermore, human bones can be differentiated from non-human remains. This study will focus on samples of human bone as well as various animal bones. The laser spectra for each species will be analyzed for outstanding elemental signatures, and then compared. Laser-Induced Breakdown Spectroscopy has the potential to advance the field of anthropology, especially in forensic and archaeological contexts, through its efficient and non-destructive elemental analysis of unknown materials.

Appendix B: Data Collection Form

Data Collection				
Donor #:			**Date Started:**	
Date	**Bone/Shot Location**	**Time Stamp**	**Notes**	**Revision Shot Date/Time**
	Bone 1: R Clavicle			
	1. Medial clavicle, inferior			
	2. Anterior midpoint			
	3. Anterior acromial third			
	4. Superior acromial third			
	5. Approx. conoid tubercle			
	6. Superior midpoint			
	7. Anterior medial third			
	8. Medial surface			
	9. Lateral clavicular facet			
	Bone 2: R Scapula			
	1. Inferior angle of infraspinatus fossa			
	2. Infraspinous fossa			
	3. Infraspinous fossa towards medial border			
	4. Superior angle of subscapularis fossa			
	5. Glenoid fossa			
	6. Superior aspect of acromial process			
	7. Inferior angle on anterior side			
	8. Anterior side of lateral border			
	9. Middle of subscapularis fossa			
	10. Coracoid process			
	Bone 3: R Humerus			
	1. Humeral head			
	2. Greater tubercle			
	3. Posterior side of proximal third of diaphysis			
	4. Anterior side of midshaft			
	5. Posterior distal end, approximately olecranon fossa			
	6. Superior to coronoid fossa			
	7. Capitulum			
	8. Posterior proximal third			
	9. Medial epicondyle			

	Bone 4: R Ulna			
	1. Olecranon process			
	2. Proximal third diaphysis, posterior side			
	3. Posterior midpoint of diaphysis			
	4. Distal third diaphysis			
	5. Distal third			
	6. Distal third, 2nd area			
	7. Proximal third, medial side			
	8. Distal epiphysis			
	9. Styloid process			
	Bone 5: R Radius			
	1. Radial head			
	2. Radial tuberosity			
	3. Midshaft			
	4. Distal third anterior			
	5. Distal third posterior			
	6. Distal epiphysis			
	7. Anterior midshaft			
	Bone 6: R MC1			
	1. Head			
	2. Dorsal surface towards head			
	3. Dorsal surface towards base			
	Bone 7: R Proximal MC1 phalanx			
	1. Head			
	2. Dorsal surface towards base			
	3. Mid-dorsal surface			
	Bone 8: R Distal MC1 phalanx			
	1. Middle dorsal surface			
	2. Base			
	Bone 9: R Femur			
	1. Head			
	2. Inferior part of femoral head			
	3. Greater trochanter			
	4. Proximal third of diaphysis, anterior			
	5. Proximal third, medial side			
	6. Proximal third, anterior			
	7. Middle anterior			
	8. Distal third, anterior			
	9. Distal third, lateral			
	10. Posterior distal third			
	11. Medial condyle			

	12. Lateral condyle			
	13. Proximal third, lateral side			
	14. Lesser trochanter			
	Bone 10: R Tibia			
	1. Lateral condyle			
	2. Medial condyle			
	3. Fibular articular facet, proximal			
	4. Posterior proximal third			
	5. Posterior proximal third, lateral			
	6. Posterior proximal third, medial			
	7. Distal third, medial			
	8. Medial malleolus			
	9. Distal epiphysis, posterior			
	10. Distal epiphysis, lateral			
	Bone 11: Cranium			
	1. Frontal			
	2. Bregma			
	3. Lambda			
	4. R parietal			
	5. L parietal			
	6. L temporal			
	7. R temporal			
	8. Occipital, L portion			
	9. Maxillary M2 crown			
	10. External occipital protuberance			
	11. R maxilla, near zygomatic			
	Bone 12: Mandible			
	1. Mental eminence			
	2. R horizontal ramus			
	3. R vertical ramus, medial surface			
	4. L horizontal ramus			
	5. Mandibular R canine #27			
	6. R 2nd premolar			
	7. 1st molar, R			
	8. L canine			
	9. 2nd premolar, L			
	10. Mental eminence, inferior side			
	Bone 13: R Fibula			
	1. Lateral malleolus			
	2. Distal third, medial			
	3. Distal third, lateral			
	4. Midshaft			
	5. Proximal third			

	6. Proximal fibular facet			
	Bone 14: R Calcaneus			
	1. Calcaneal tuberosity			
	2. Sustentacular tali			
	3. Talar facet			
	4. Calcaneal tuberosity, inferior			
	Bone 15: 1st MT			
	1. Head			
	2. Superior midshaft			
	3. Plantar aspect of base			
	4. Midshaft, lateral			
	5. Facet of base			
	Bone 16: 1st MT Proximal Phalanx			
	1. Plantar aspect of base			
	2. Articular surface of head			
	3. Superior portion of base			
	Bone 17: Distal Phalanx MT1			
	1. Articular facet of the base			
	2. Midshaft plantar aspect			
	3. Apical tuft			
	Bone 18: R 1st Rib			
	1. Inferior aspect of sternal end			
	2. Inferior aspect of the angle			
	3. Inferior aspect adjacent to the tubercle			
	4. Tubercle			
	5. Superior aspect of the angle			
	Bone 19: R 2nd Rib			
	1. The angle			
	2. Midpoint			
	3. Rib head			
	4. Superior part of sternal end			
	Bone 20: R Innominate			
	1. Lateral aspect of iliac blade near iliac crest			
	2. Lateral aspect of posterior superior iliac spine			
	3. Lateral aspect of posterior inferior iliac spine			
	4. Lateral aspect of iliac tuberosity			
	5. Ischial tuberosity			
	6. Dorsal aspect of pubis			
	7. Anterior superior iliac spine			

	8. Pubic symphysis			
	9. Auricular surface			
	10. Acetabular margin			
	Bone 21: Sacrum			
	1. Anterior aspect of S1, midline			
	2. Auricular surface, R			
	3. Facet for coccyx			
	4. R ala			
	5. Superior part of the body			
	Bone 22: C2			
	1. Articular facet on R			
	2. Articular facet on L			
	3. Dens			
	4. Anterior aspect of body			
	5. L lamina			
	Bone 23: T10			
	1. Inferior aspect of the body			
	2. Superior			
	3. Tip of spinous process			
	4. L tip of transverse process			
	Bone 24: L humerus			
	1. Humeral head			
	2. Greater tubercle			
	3. Posterior side of proximal third of diaphysis			
	4. Anterior side of midshaft			
	5. Posterior distal end, approximately olecranon fossa			
	6. Superior to coronoid fossa			
	7. Capitulum			
	8. Posterior proximal third			
	9. Medial epicondyle			
	Bone 25: L Ulna			
	1. Olecranon process			
	2. Proximal third diaphysis			
	3. Posterior midpoint of diaphysis			
	4. Distal third diaphysis, medial			
	5. Distal third			
	6. Distal third			
	7. Distal epiphysis			
	8. Proximal third, medial side			
	9. Styloid process			
	Bone 26: L Radius			

	1. Radial head			
	2. Radial tuberosity			
	3. Midshaft			
	4. Distal third anterior			
	5. Distal third posterior			
	6. Distal epiphysis			
	7. Anterior midshaft			
	Bone 27: L Femur			
	1. Head			
	2. Inferior part of femoral head			
	3. Greater trochanter			
	4. Proximal third of diaphysis, anterior			
	5. Proximal third, medial side			
	6. Proximal third, anterior			
	7. Middle anterior			
	8. Distal third, anterior			
	9. Distal third, lateral			
	10. Posterior distal third			
	11. Medial condyle			
	12. Lateral condyle			
	13. Proximal third, lateral side			
	14. Lesser trochanter			
	Bone 28: L Tibia			
	1. Lateral condyle			
	2. Medial condyle			
	3. Fibular articular facet, proximal			
	4. Posterior proximal third			
	5. Posterior proximal third, lateral			
	6. Posterior proximal third, medial			
	7. Distal third, medial			
	8. Medial malleolus			
	9. Distal epiphysis, posterior			
	10. Distal epiphysis, lateral			
	Bone 29: L Fibula			
	1. Lateral malleolus			
	2. Distal third, medial			
	3. Distal third, lateral			
	4. Midshaft			
	5. Proximal third			
	6. Proximal fibular facet			
	Additional Bone(s):			

Appendix C: Averaged Spectra for Each Donor.

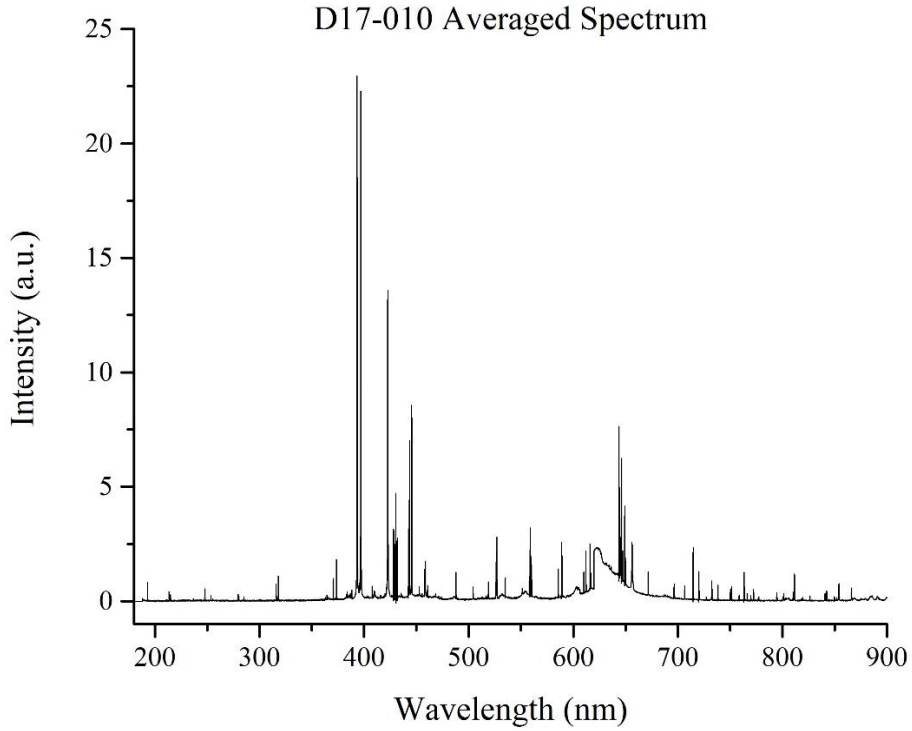

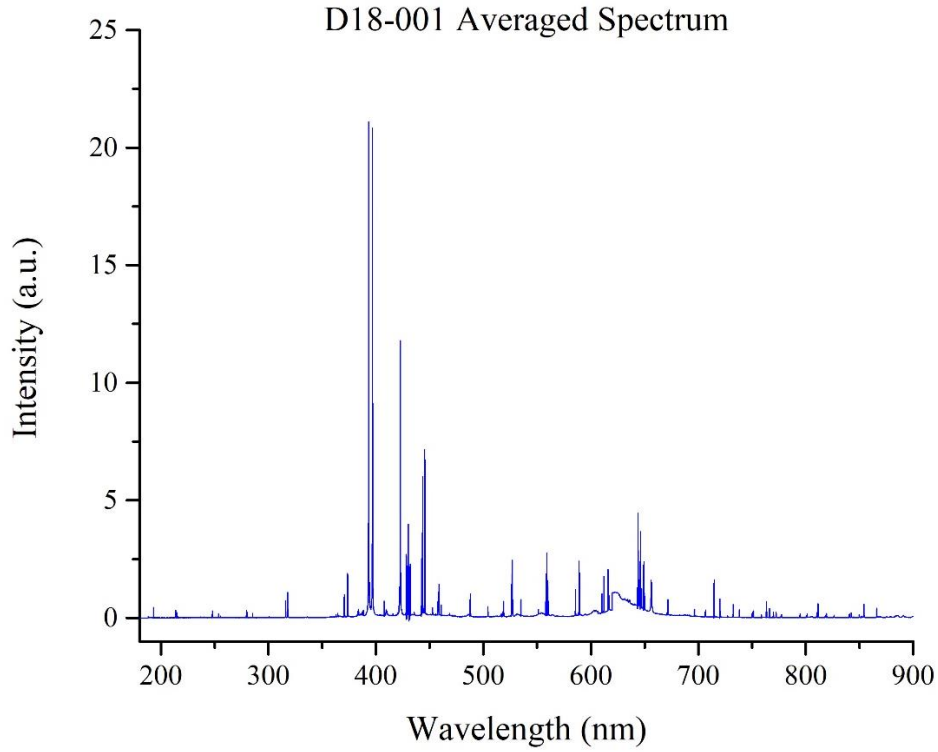

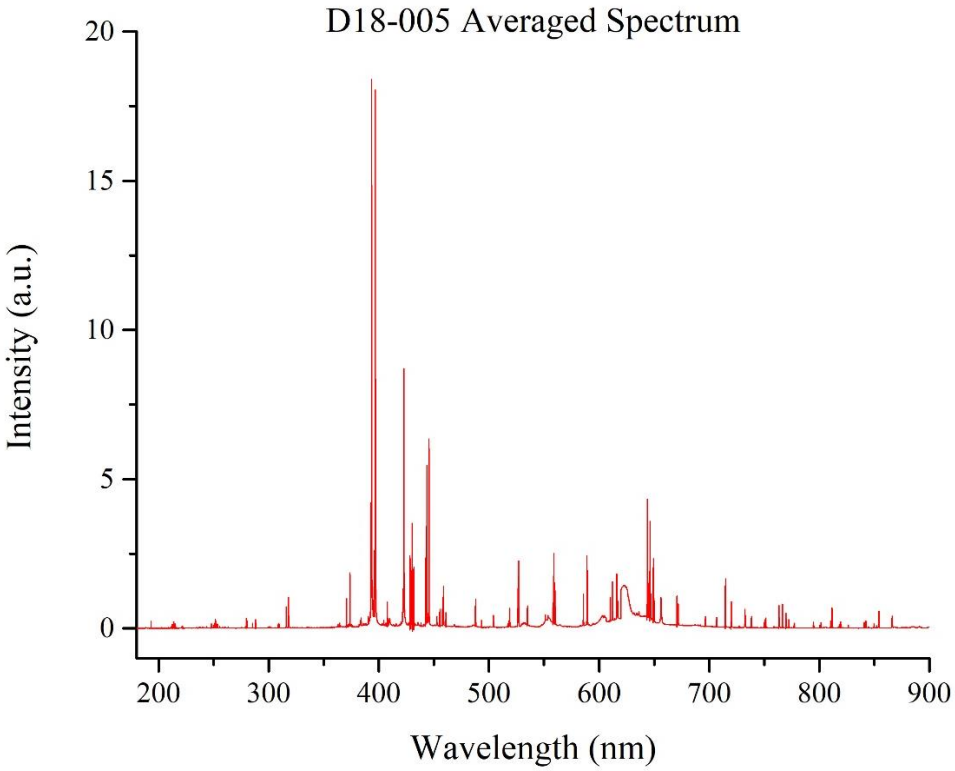
D18-005 Averaged Spectrum
Intensity (a.u.)
Wavelength (nm)
0
5
10
15
20
200
300
400
500
600
700
800
900

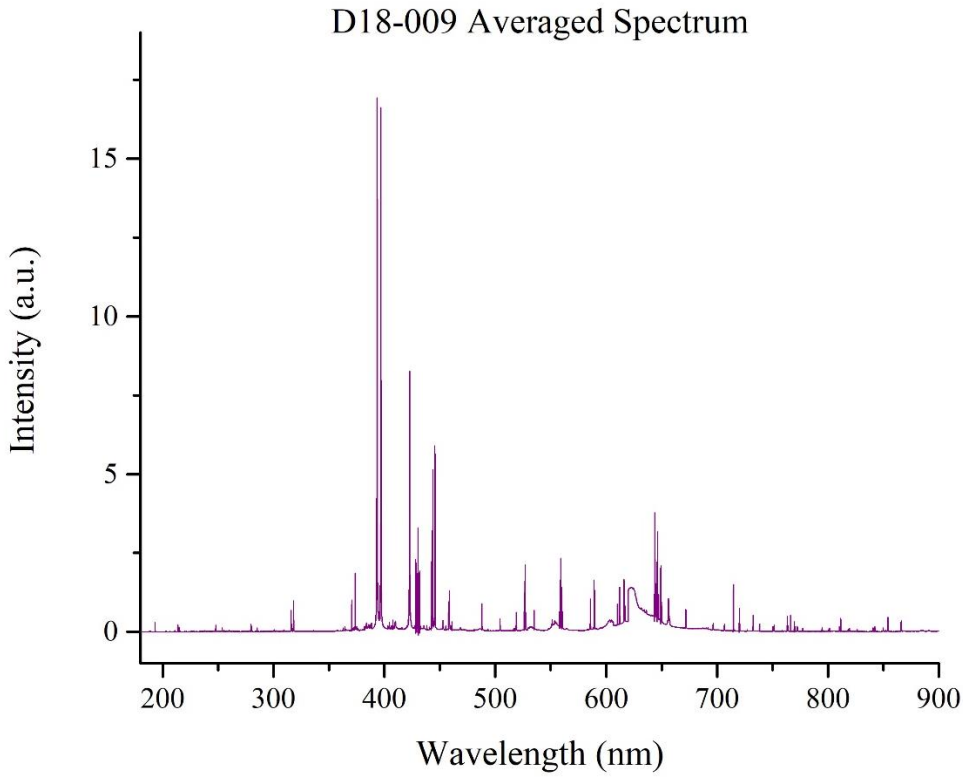
D18-009 Averaged Spectrum
Intensity (a.u.)
Wavelength (nm)
0
5
10
15
200
300
400
500
600
700
800
900

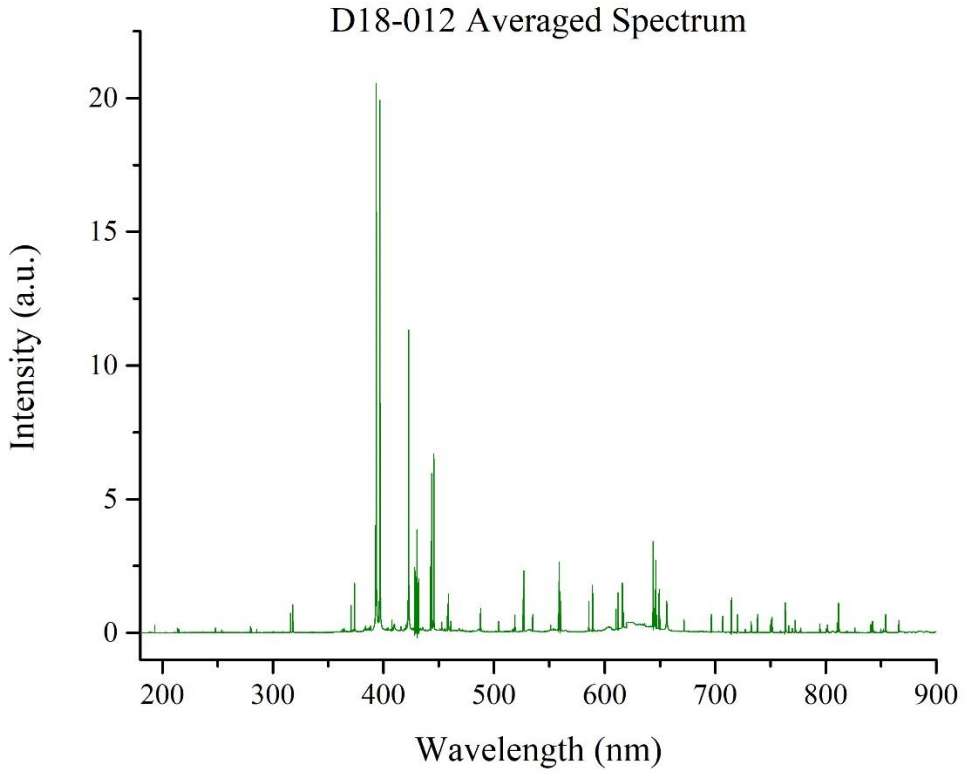
D18-012 Averaged Spectrum
Intensity (a.u.)
0
5
10
15
20
200
300
400
500
600
700
800
900
Wavelength (nm)

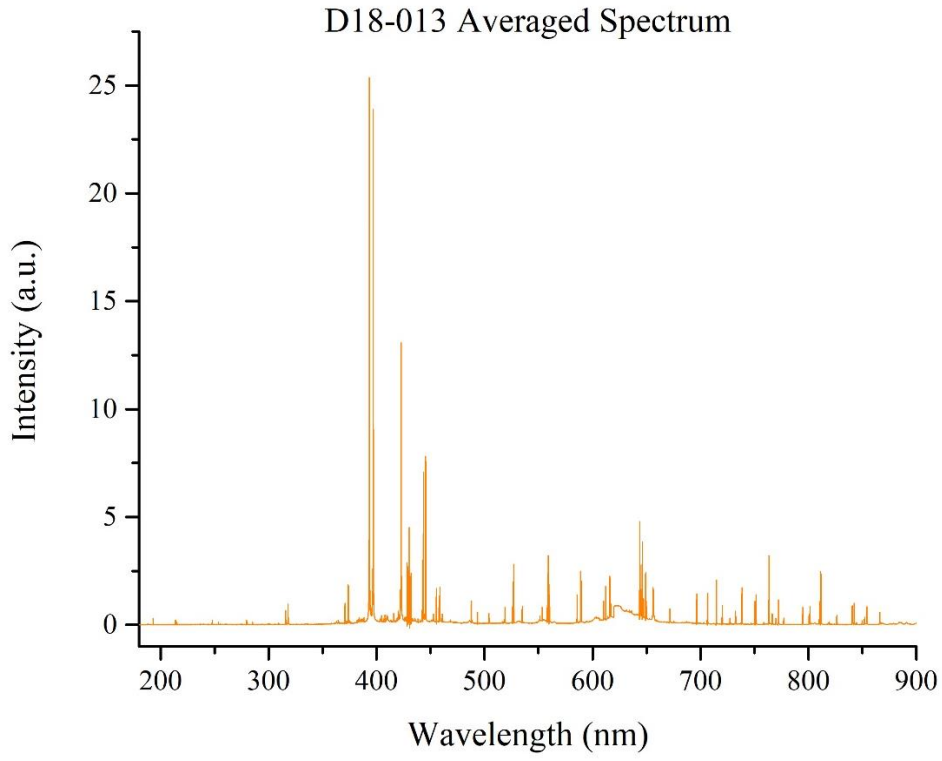
D18-013 Averaged Spectrum
Intensity (a.u.)
0
5
10
15
20
25
200
300
400
500
600
700
800
900
Wavelength (nm)

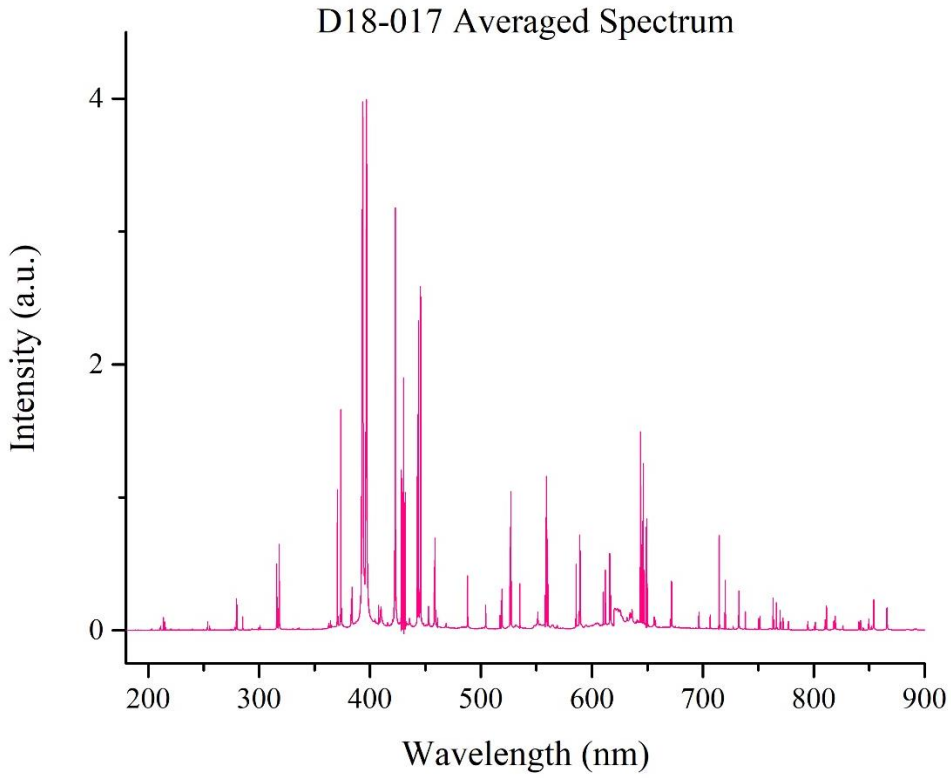
D18-017 Averaged Spectrum
Intensity (a.u.)
0
2
4
200
300
400
500
600
700
800
900
Wavelength (nm)

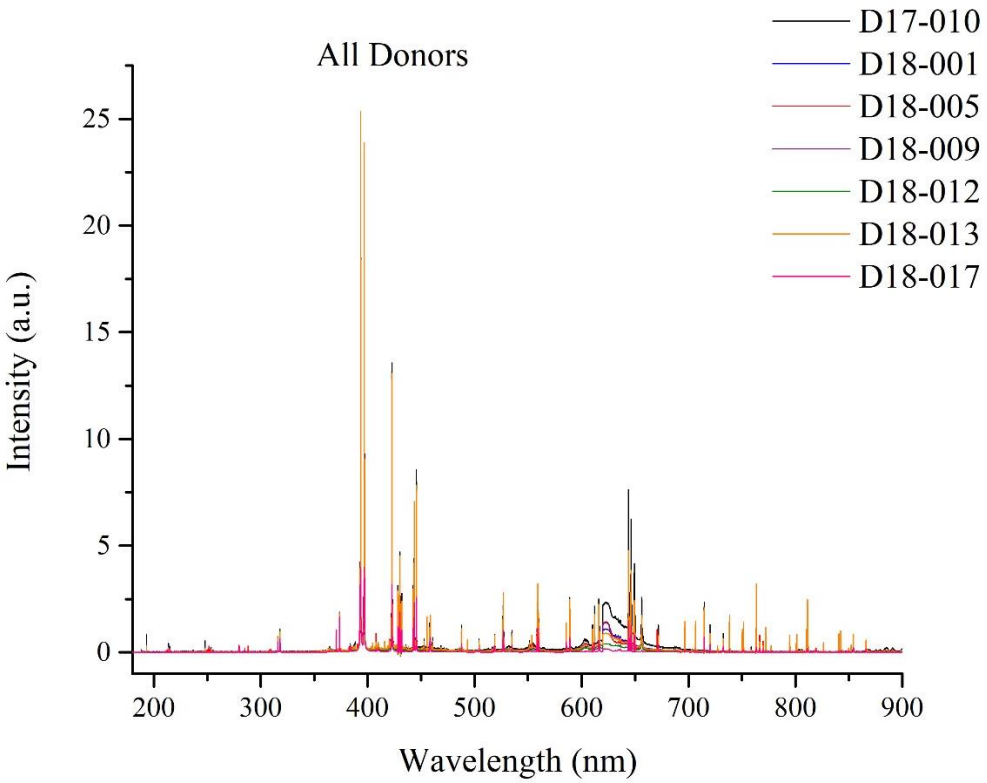
All Donors
D17-010
D18-001
D18-005
D18-009
D18-012
D18-013
D18-017
Intensity (a.u.)
0
5
10
15
20
25
200
300
400
500
600
700
800
900
Wavelength (nm)